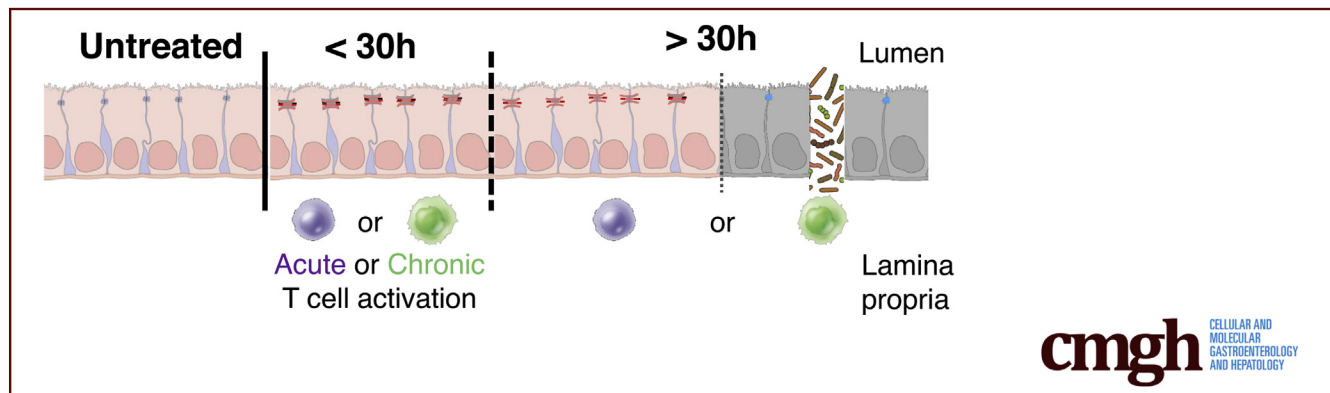


ORIGINAL RESEARCH

Regulation of Intestinal Epithelial Barrier and Immune Function by Activated T Cells

Nga Le,¹ Claire Mazahery,² Kien Nguyen,¹ and Alan D. Levine^{1,2,3,4,5,6}

¹Department of Molecular Biology and Microbiology; ²Department of Pathology; ³Department of Pharmacology; ⁴Department of Medicine; ⁵Department of Pediatrics; and ⁶Case Comprehensive Cancer Center, Case Western Reserve University, Cleveland, Ohio



SUMMARY

Bidirectional communication between T lymphocytes and the intestinal epithelium is intricately controlled in health and disease. Activated T cells modulate biphasic epithelial permeability by regulating tight junction expression, assembly, and cell morphology. In response, the epithelium alters its synthesis of immune mediators.

BACKGROUND & AIMS: Communication between T cells and the intestinal epithelium is altered in many diseases, causing T-cell activation, depletion, or recruitment, and disruption of the epithelium. We hypothesize that activation of T cells regulates epithelial barrier function by targeting the assembly of the tight junction complex.

METHODS: In a 3-dimensional and 2-dimensional co-culture model of activated T cells subjacent to the basolateral surface of an epithelial monolayer, the pore, leak, and unrestricted pathways were evaluated using transepithelial resistance and flux of fluorescently labeled tracers. T cells were acutely and chronically activated by cross-linking the T-cell receptor. Tight junction assembly and expression were measured using quantitative polymerase chain reaction, immunoblot, and immunofluorescence confocal microscopy.

RESULTS: Co-culture with acutely and chronically activated T cells decreased the magnitude of ion flux through the pore pathway, which was maintained in the presence of acutely activated T cells. Chronically activated T cells after 30 hours induced a precipitous increase in the magnitude of both ion and molecular flux, resulting in an increase in the unrestricted

pathway, destruction of microvilli, expansion in cell surface area, and cell death. These fluctuations in permeability were the result of changes in the assembly and expression of tight junction proteins, cell morphology, and viability. Co-culture modulated the expression of immune mediators in the epithelium and T cells.

CONCLUSIONS: Bidirectional communication between T cells and epithelium mediates a biphasic response in barrier integrity that is facilitated by the balance between structural proteins partitioning in the mobile lateral phase vs the tight junction complex and cell morphology. (*Cell Mol Gastroenterol Hepatol* 2021;11:55–76; <https://doi.org/10.1016/j.jcmgh.2020.07.004>)

Keywords: Claudin; Occludin; Paracellular Permeability; Pore Pathway; Leak Pathway.

The epithelium of the gastrointestinal tract, created by a monolayer of polarized intestinal epithelial cells (IECs), serves as a nonpenetrable microbial barrier and a selectively permeable filter for water, ion, nutrient absorption, and waste secretion. Tight junctions (TJs) seal the monolayer and regulate paracellular intestinal permeability by forming a belt-like network of contact points that surround each cell, attaching it to neighboring cells.¹ In addition to its barrier function, the TJ acts to transfer bidirectional signals between the interior and exterior environment, which regulates TJ assembly and function and, consequently, permeability.²

TJs are assembled from transmembrane proteins that include members of the large claudin protein family and

occludin. Some claudin proteins create paracellular channels, whereas other claudins and occludin seal the intercellular space.^{3,4} Other integral membrane proteins, such as the zonula occludens (ZO), also function to regulate and maintain epithelial permeability.⁵ Permeability is controlled by paracellular flux through 2 distinct mechanisms: the pore and leak pathways.^{6,7} The pore pathway is size- and charge-selective, transporting molecules with a maximal diameter from approximately 0.5 nm to approximately 1 nm.⁸ The leak pathway is not charge-selective, limited in capacity, allowing molecules with diameters up to 10 nm to pass.⁹ When the epithelium is damaged, large molecules and microbes can easily cross the barrier via a route termed the *unrestricted pathway*.¹⁰

The epithelial monolayer also plays a pivotal role in innate and adaptive immunity. IECs are in continuous communication with subjacent immune cells, ensuring the maintenance of a healthy and immunologically protective physical barrier.¹¹ When stimulated by pathogenic microbes or inflammatory signals from immune cells, IECs secrete cytokines and chemokines and express cytokine receptors, showing that IECs respond to and regulate mucosal immune cells.¹² IECs also present antigenic peptides to both CD4+ and CD8+ T lymphocytes, priming the immune system by triggering the activation of dendritic cells, T cells, and B cells.¹³ Complementing the physical epithelial barrier, T lymphocytes in the underlying lamina propria orchestrate the second line of defense and maintain gut homeostasis. Mucosal T cells show an activated phenotype, but concurrently have reduced proliferative capacity and cytokine production,¹⁴ enabling them to maintain an equilibrium between effective immunity and physiologic immune tolerance to preserve tissue homeostasis in the presence of commensal microflora.¹⁵ Thus, mucosal T cells support immunologic protection without compromising organ integrity. The origin of a mucosal T cell is via the activation of circulating naïve T cells as they transit into intestinal lymphoid tissues, such as Peyer's patches, lymphoid follicles, and mesenteric lymph nodes. These educated T cells then home to the lamina propria and adopt their mucosal phenotype.

Disruption of communication between T cells and IECs is associated with many chronic diseases, including inflammatory bowel disease (IBD), whose pathogenesis is linked to excessive activity of mucosal T cells and a defect in tolerance mechanisms mediated by resident and infiltrating T cells. Mucosal inflammation in IBD is accompanied by the activation and proliferation of peripheral T cells, resulting from increased intestinal permeability, epithelial cell apoptosis, and consequent translocation of microbial products into lamina propria and circulation.¹⁶ However, the mechanism by which T cells communicate with the epithelium and maintain barrier integrity is poorly understood. We therefore hypothesize that activated T cells modulate the barrier function of the intestinal epithelium by controlling the expression, location, and assembly of the protein subunits of the paracellular tight junctional complex.

The goal of this study was to investigate the bidirectional communication between activated T cells and IECs and identify the mechanisms by which T cells regulate paracellular permeability and modulate barrier integrity. We developed an

in vitro 2-dimensional (2-D) and a 3-dimensional (3-D) co-culture model, which were used to show that activated T lymphocytes initiate a response in the epithelium that initially increases barrier integrity. This enhanced barrier function is either maintained or rapidly reversed, depending on the duration of the initial T-cell receptor stimulus and whether synthesis of the resulting cytokines is transient or continuous. Persistently activated T cells, which maintain continued cytokine production, promote paracellular permeability in the epithelium by disassembling the TJ, reducing the IEC proliferation, and inducing cell death.

Results

Polarized IECs Attract the Migration of Activated T Cells

To investigate the capability of an IEC monolayer to modulate the migration of blood-derived T cells into sites of mucosal inflammation, we developed a 3-D, colonoid-like co-culture model. The human intestinal epithelial Caco-2 cell subclone brush border expressing clone (BBE) was cultured in Matrigel (Corning, Corning, NY) to support the formation of organoid-like cysts surrounded by a single layer of polarized IECs (Figure 1A and B). Human peripheral blood CD3+ T cells were activated by cross-linking the T-cell receptor with anti-CD3/CD28 beads. The epithelial culture was overlaid with a thin layer of Matrigel containing activated T cells (Figure 1A). After 2 days, pulse-activated T cells migrate into the spheroid-containing layer and establish a close and continuous interaction with the basolateral surface of the epithelial monolayer (Figure 1C). In contrast, persistently activated T cells migrate more slowly, and, after 2 days, only a small number were detected in the lower Matrigel layer, and few were associated with the cysts (Supplementary Movies 1, 2, and 3).

Persistently Activated T Cells Disrupt the Permeability of an IEC Monolayer

We investigated the ability of these T cells to modulate the permeability of the epithelial barrier, recording the flux of fluorescein isothiocyanate-labeled 4-kilodalton dextran (FD4) from the basolateral surface to the cyst apical lumen by quantitative confocal microscopy. Pulse-activated T cells induced a minimal increase in FD4 flux to the apical lumen

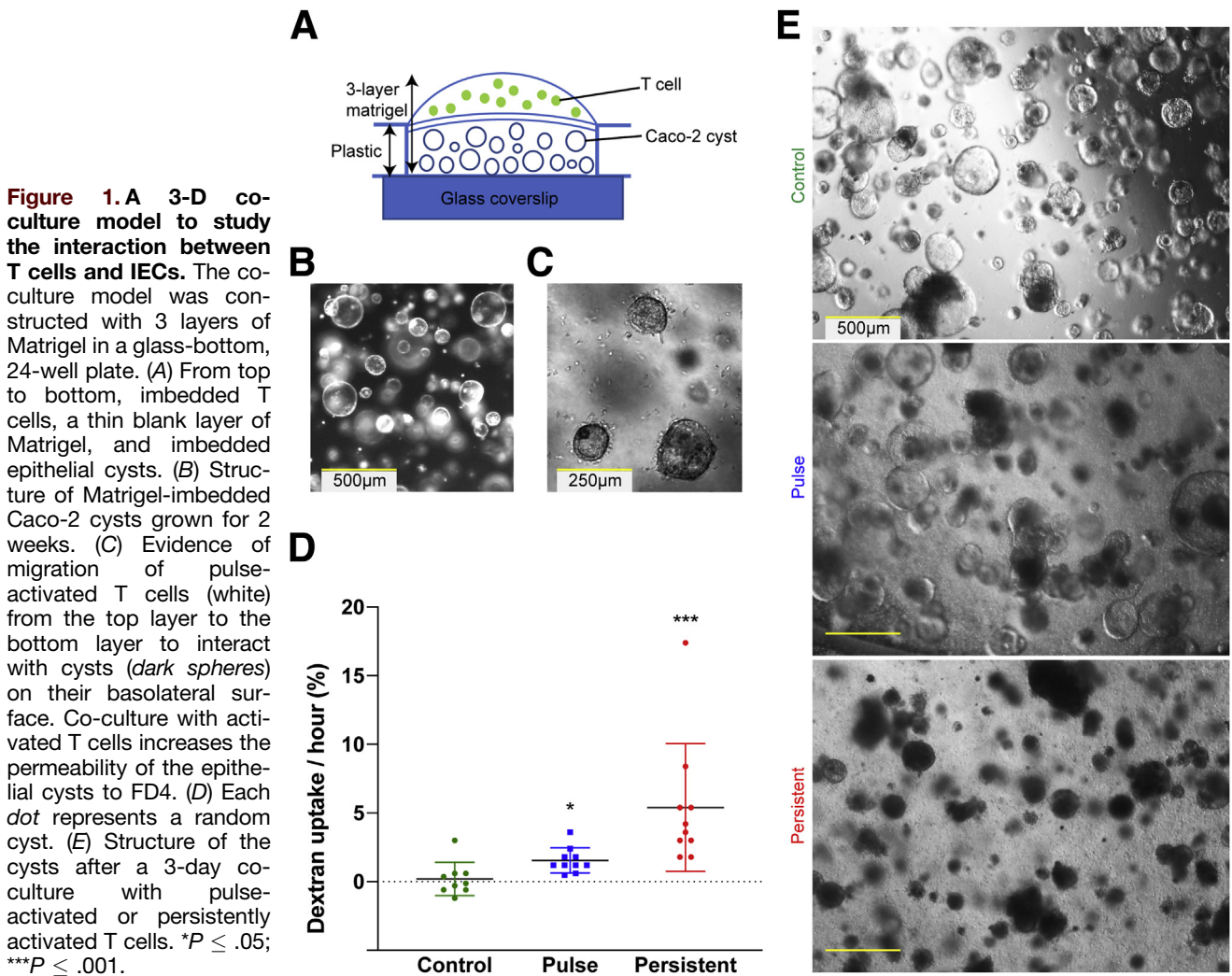
Abbreviations used in this paper: BBE, brush border expressing clone; B2M, β 2-microglobulin; CLDN, claudin; FD4, fluorescein isothiocyanate-labeled 4-kilodalton dextran; HBSS, Hank's balanced salt solution; IBD, inflammatory bowel disease; IEC, intestinal epithelial cell; IFN- γ , interferon- γ ; IL, interleukin; MHC, major histocompatibility complex; mRNA, messenger RNA; PBS, phosphate-buffered saline; PD-1, programmed death 1; PD-L1, programmed death ligand 1; TER, transepithelial electrical resistance; TGF- β , transforming growth factor- β ; 3-D, 3-dimensional; TJ, tight junction; TNF- α , tumor necrosis factor- α ; 2-D, 2-dimensional; ZO, zonula occludens.

 Most current article

© 2020 The Authors. Published by Elsevier Inc. on behalf of the AGA Institute. This is an open access article under the CC BY-NC-ND license (<http://creativecommons.org/licenses/by-nc-nd/4.0/>).

2352-345X

<https://doi.org/10.1016/j.jcmgh.2020.07.004>



over 3 hours (Figure 1D), with no evidence of harm to the epithelium after 3 days (Figure 1E). In contrast, persistently activated T cells dramatically increased FD4 flux (Figure 1D), explained by partial breakdown in cyst structure, decreased translucence, and epithelial cell death (Figure 1E).

To define the mechanism by which activated T cells modulate barrier integrity, we cultured Caco-2 BBe cells in an inverse configuration on a semipermeable filter in a Transwell culture dish (Figure 2A), creating a polarized monolayer in which the upper chamber is adjacent to the basolateral surface. Both pulse-activated and persistently activated human T cells added to the upper chamber stimulated a steady increase in transepithelial electrical resistance (TER) between 15 and 24 hours of co-culture, signifying a reduction in ion flux across the barrier (Figure 2B). Once maximal resistance was reached, monolayers co-cultured with pulse-activated T cells sustained this increased level of resistance, while monolayers co-cultured with persistently activated T cells initiated a second phase of the response, in which there was a continuous decrease in

resistance over the following 4 days, often decreasing to below the control level (Figure 2B). This biphasic response was observed with all donors (2 representative donors shown), therefore it is not dependent on a major histocompatibility complex (MHC) match between IECs and T cells. The addition of anti-CD3/CD28 Dynabeads alone to the monolayer had no effect on TER (Figure 3A). We will refer to phase 1 as when the TER increases within the first 30 hours in response to all activated T cells, and phase 2 is defined by the steady-state resistance maintained by pulse-activated T cells or the decrease in resistance induced by persistently activated T cells.

To evaluate the leak pathway, T cells were removed at the end of phase 1 or phase 2 and a mixture of fluorescein and fluorescently labeled dextrans of different molecular weight, and hence diameter, were added to the basolateral chamber. When the leak pathway was analyzed as apparent permeability, an untreated monolayer was slightly permeable to fluorescein (11 Å) and 3.5 kilodaltons dextran (28 Å), and impermeable to 70 kilodaltons dextran (116 Å) (Figure 3B). There was no noticeable difference in the rate

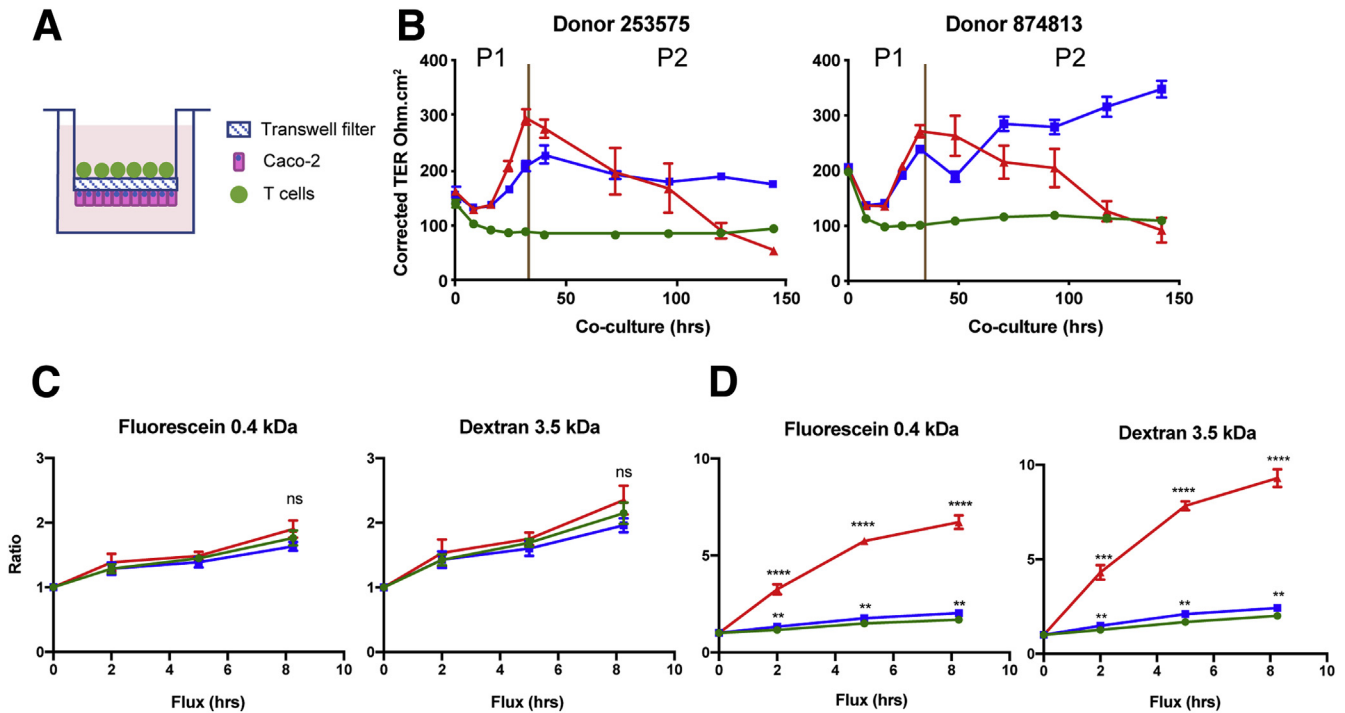


Figure 2. Activated T cells modulate the pore and leak permeability pathways of an intestinal epithelial cell monolayer in a 2-D co-culture model. (A) A 2-D, anatomically correct, co-culture model of a Transwell filter coated with a polarized monolayer. (B) Pulse-activated (blue) and persistently activated (red) T cells induce a biphasic response on the TER vs a control (green) monolayer, independent of T-cell donor (P1, phase 1; P2, phase 2). (C) The ratio of normalized fluorescent intensity for the passage of fluorescein (11 Å) and dextran 3.5 kilodaltons (28 Å) relative to the flux intensity of 116 Å dextran 70 kilodaltons was unchanged by co-culture with pulse-activated or persistently activated T cells in phase 1. (D) Persistently activated T cells induce a significantly higher rate of fluorescein and dextran 3.5 kilodaltons flux relative to dextran 70-kilodalton flux in phase 2. ns, $P \geq .05$; ** $P \leq .01$; *** $P \leq .001$; **** $P \leq .0001$.

of passage of any probe between untreated and activated T-cell-exposed IECs in phase 1 (Figure 3B). Because the untreated monolayer allows limited small-molecule permeability at baseline, co-culture with activated T cells could not increase its barrier strength further, as was observed in phase 1 for the pore pathway. At the end of phase 2, pulse-activated T cells, which sustain increased TER (ie, reduced ion flux via the pore pathway), induced a minimal increase in leak pathway permeability for smaller probes (11 and 28 Å) and had no effect when evaluated with the larger probe (116 Å) (Figure 3C). In contrast, persistently activated T cells in phase 2 induced extremely high apparent permeability through the epithelium for all size ranges, noting, in particular, permeability for a 70-kilodalton probe, which measures the unrestricted pathway. To evaluate if the increase in apparent permeability of the smaller probes in the persistently activated T cell co-culture is owing to increased damage to the barrier and thus passage through the unrestricted pathway, we determined the ratio of the levels of fluorescein or 3.5 kilodaltons dextran flux relative to 70 kilodaltons dextran flux (Figure 2C and D). Consistent with measurements of apparent permeability, the net flux of all probes was not affected by T cell co-culture in phase 1 (Figure 3B and D), whereas the increased permeability of both smaller probes in phase 2, when the monolayer was co-cultured with persistently activated T cells

(Figure 3C and E), was indeed mediated by passage through the leak and unrestricted pathway (Figure 3B). Thus, sustained contact with persistently activated T cells, modeling chronically inflamed T cells, damages the barrier, dysregulating the flux of ions and macromolecules.

Defining the Activation Status of Pulse-Activated and Persistently Activated T Cells

To characterize the immunologic properties that distinguish the pulse-activated from persistently activated T-cell population, we evaluated their proliferative capacity, predisposition toward apoptosis, cytokine synthesis profile, and homing capabilities after co-culture with IECs during both phase 1 and phase 2. Setting input T cells immediately after activation as control, both pulse-activated and persistently activated T cells during phase 1 express similar levels of Ki67 messenger RNA (mRNA) ($124\% \pm 8.08\%$ and $116\% \pm 8.79\%$ of control, respectively). However, in phase 2, pulse-activated T cells show significant 7-fold-reduced Ki67 mRNA levels ($13.7\% \pm 1.93\%$), whereas Ki67 expression in persistently activated T cells remains relatively unchanged at $86.7\% \pm 7.68\%$. These findings suggest that pulse-activated T cells become quiescent in phase 2, while persistently activated T cells remain stimulated. To assess if these T cells are undergoing

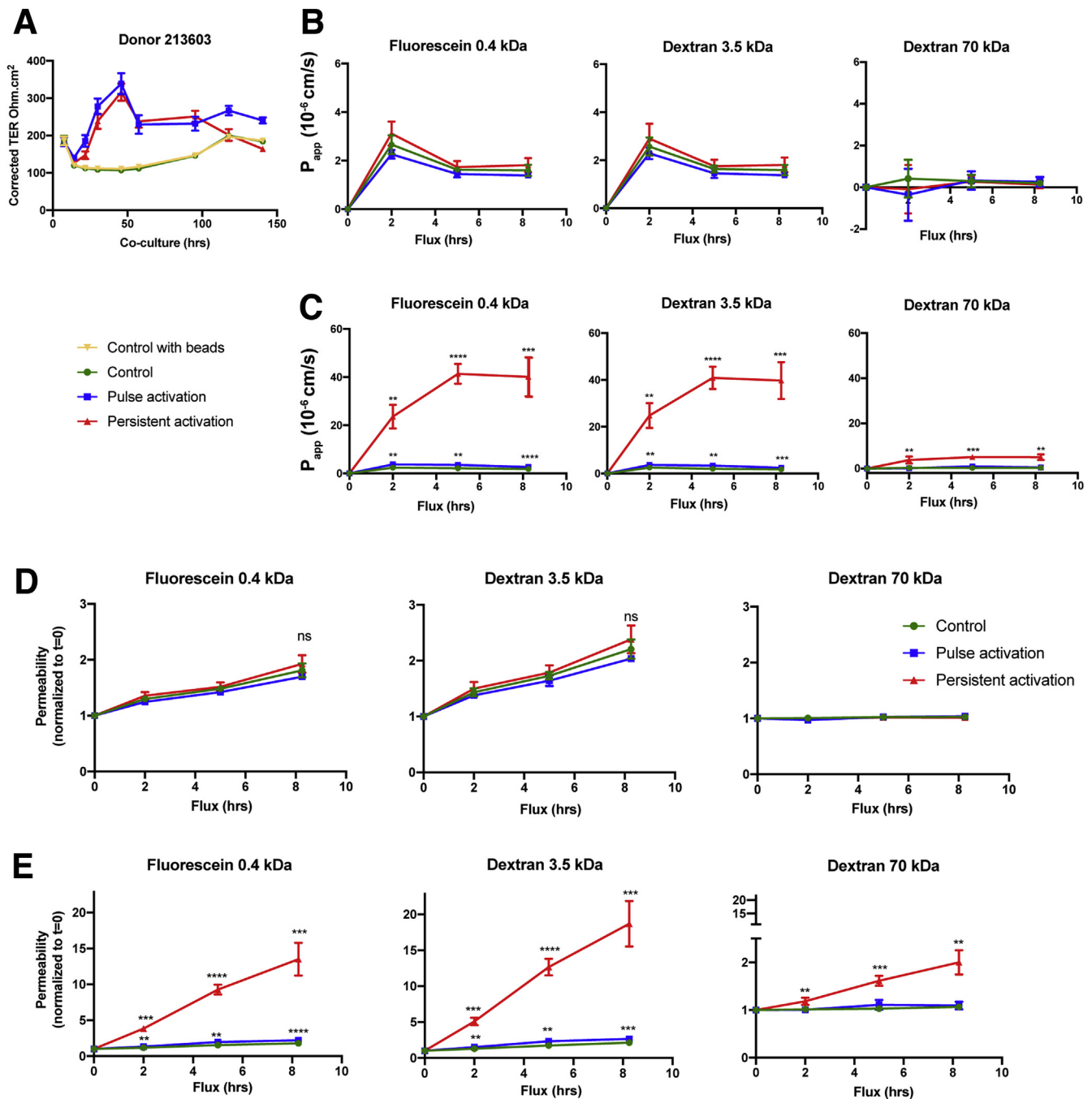


Figure 3. Activated T cells modulate the pore, leak, and unrestricted paracellular permeability pathways of an intestinal epithelial cell monolayer. (A) Although pulse-activated (blue) and persistently activated (red) T cells induce a biphasic response in an epithelial monolayer, adding anti-CD3/CD28 Dynabeads alone (gold) to the Transwell culture had no effect on TER. (B–E) The permeability of the epithelial barrier was evaluated by following the paracellular flux of fluorescent probes. Pulse-activated (blue) and persistently activated (red) T cells do not modulate the passage of small (11 Å), medium (28 Å), and large (116 Å) probes vs a control (green) monolayer in phase 1 (B), while persistently activated T cells significantly increased the apparent permeability (P_{app}) of all 3 probes in phase 2 (C). The net flux of the fluorescently labeled tracers, normalized to $t = 0$, is shown for phase 1 (D) and phase 2 (E). ns, $P > .05$; $**P \leq .01$; $***P \leq .001$; $****P \leq .0001$.

apoptosis, their live/dead ratio was determined by flow cytometry. The percentage of dead cells remains consistently at less than 4% through the co-culture in all T-cell subtypes (data not shown), indicating that cell death is unlikely to contribute to the decrease of barrier integrity in phase 2 for persistently activated T cells.

As expected, activating T cells by cross-linking CD3/CD28 induced expression of the cell surface markers CD69 and CD25, and their surface expression levels remained increased in phase 1 for both T-cell subtypes (Figure 4A). Consistent with the loss of proliferative potential of pulse-activated T cells in phase 2, CD69 and CD25 levels begin

to return to baseline, while these activation markers remain high in persistently activated T cells (Figure 4A). Furthermore, mRNA expression of the activation marker programmed death 1 (PD-1) followed the same kinetic response (data not shown). In phase 1, the ratio of CD4+ to CD8+ T cells remained unchanged, whereas in phase 2 the ratio of CD4+ to CD8+ decreased from 1.6 to 1.2 for pulse activation co-cultures and increased to 2.0 in persistent activation co-cultures. Pulse and persistent activation co-culture with the monolayer slightly favored the expansion of CD8+ T cells and the decrease of CD8+ T cells, respectively, in phase 2. These results, together with those discussed below, suggest there is reciprocal communication between T cells and IECs.

We investigated the expression of homing markers and chemokine receptors on activated T cells to potentially explain their migration pattern. The mean fluorescent intensity of the gut-homing integrin $\beta 7$ immediately after activation was increased modestly, and this increase remained constant throughout co-culture. The percentage of pulse-activated T cells expressing integrin $\beta 7$ also increased in both phase 1 and phase 2, although this increase was not observed for persistently activated T cells, suggesting increased homing potential for pulse-activated cells (Figure 4A). We detected a similar increase in migration potential for pulse-activated T cells when measuring mRNA levels for $\beta 7$, CD11a (integrin αL), and C-C Motif Chemokine Receptor 9, whose levels decreased in persistently activated T cells (Figure 5A). This result is consistent with the migration pattern seen in the 3-D co-culture (Figure 1 and Supplementary Movie 2) in which pulse-activated T cells showed a higher capacity to migrate to the colonic organoids.

The functional consequence of T-cell activation was evaluated by measuring a wide range of cytokine mRNA synthesis after IEC T cell co-culture, normalized to an unstimulated T cell. As expected, all cytokine levels (except transforming growth factor- β [TGF- β]) were increased 10-fold or more immediately after T-cell activation (input cells). Pulse-activated T cells harvested 8 hours before the phase 1 peak had down-regulated all cytokine mRNA expression dramatically and were entirely quiescent 24 hours before the end of phase 2. In contrast, persistently activated T cells maintained increased cytokine mRNA production throughout phase 1 and only slightly decreased expression 24 hours before the end of phase 2 (Figure 4B). These results are consistent with the proliferative capacity and activation markers expression on the cells, indicating that the loss of barrier integrity in phase 2 by persistently activated T cells is associated with persistent T-cell activation. In keeping with the theme of bidirectional communication we evaluated the impact of IECs on T-cell cytokine synthesis (Figure 5B). In phase 1, Caco-2 co-culture was able to either up-regulate or down-regulate cytokine synthesis by pulse-activated T cells, while co-culture only up-regulated persistently activated T-cell cytokine expression (tumor necrosis factor- α [TNF- α], in particular). However, in phase 2, the Caco-2 monolayer down-regulated cytokine mRNA during persistent activation.

Exposure of an Epithelial Monolayer to Activated T Cells Regulates the Expression of TJ Protein and mRNA

To define the molecular mechanism that mediates changes in the pore, leak, and unrestricted pathways owing to T-cell co-culture, we evaluated the expression of key TJ proteins and mRNA in the monolayer. Claudin-1 mRNA levels modestly increase in co-culture at the peak of phase 1 after exposure to both pulse-activated and persistently activated T cells and return to baseline at the end of phase 2 (Figure 6A). In contrast, claudin-2 (Figure 6B) and occludin (Figure 6D) mRNA levels do not change during phase 1, yet are significantly higher in phase 2. Claudin-4 follows a third pattern with increased mRNA in both phases (Figure 6C). A fourth temporal pattern was shown by ZO-1, which decreased slightly in phase 1 and returned to baseline in phase 2 (Figure 6E). Gene expression changes for each of these TJ mRNAs were independent of the activation scheme for the T cells. These results show that regulation of TJ gene expression is mediated by the presence of T cells, yet because of the intricacy of the TJ complex, following a limited number of components does not capture the observed biological effect on barrier integrity.

To confirm that activated T-cell communication with an epithelial monolayer also modulates steady-state intracellular protein levels, we examined regulation by pulse-activated and persistently activated T cells of protein concentrations for the same claudin family members and occludin (Figure 6F). Co-culture with pulse-activated T cells induced higher claudin 2 and claudin 4 protein expression in phase 2, while coculture with persistently activated T cells increased claudin 2 and claudin 4 in both phases. There were no significant differences in the levels of claudin-1 between the phases or treatment regimens, however, there were more claudin-1 degradation products in phase 2 after persistent T-cell activation (Figure 6F). The expression of occludin did not change in phase 1, but increased in phase 2 on co-culture with pulse-activated T cells (Figure 6F). The lack of concordance between TJ mRNA synthesis and steady-state protein levels, in response to activated T cells, underscores the complexity of TJ regulation, assembly, degradation, and function.

Structural Changes to the TJ Complex Resulting From Activated T-Cell Engagement

Regulation of TJ protein expression does not directly address the assembled functional TJ because TJ proteins associate with the TJ complex and are found in a mobile lateral subpool that does not contribute to barrier integrity.¹ Claudin-1 and claudin-4 proteins are highly expressed in the mobile lateral subpool in a resting monolayer and were assembled into TJs in phase 1 (~3-fold increase in intensity), but not phase 2, after co-culture with either pulse-activated or persistently activated T cells (Figure 7C). By immunofluorescent staining, their total expression increased in both phases, consistent with the RNA and immunoblot data shown in Figure 6. In addition, upon T cell co-culture claudin-1 and claudin-4 showed a punctate

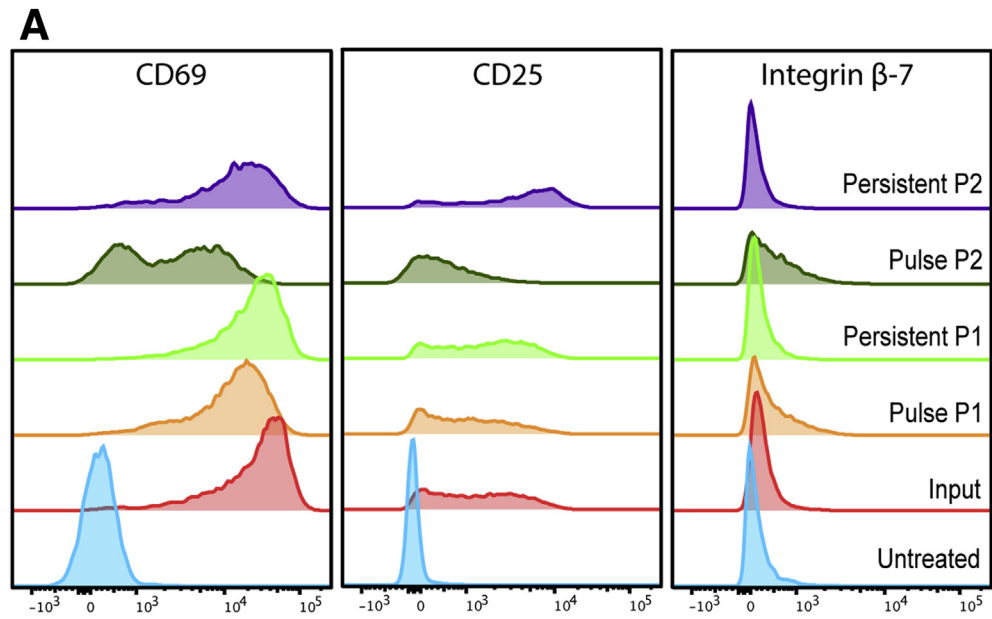
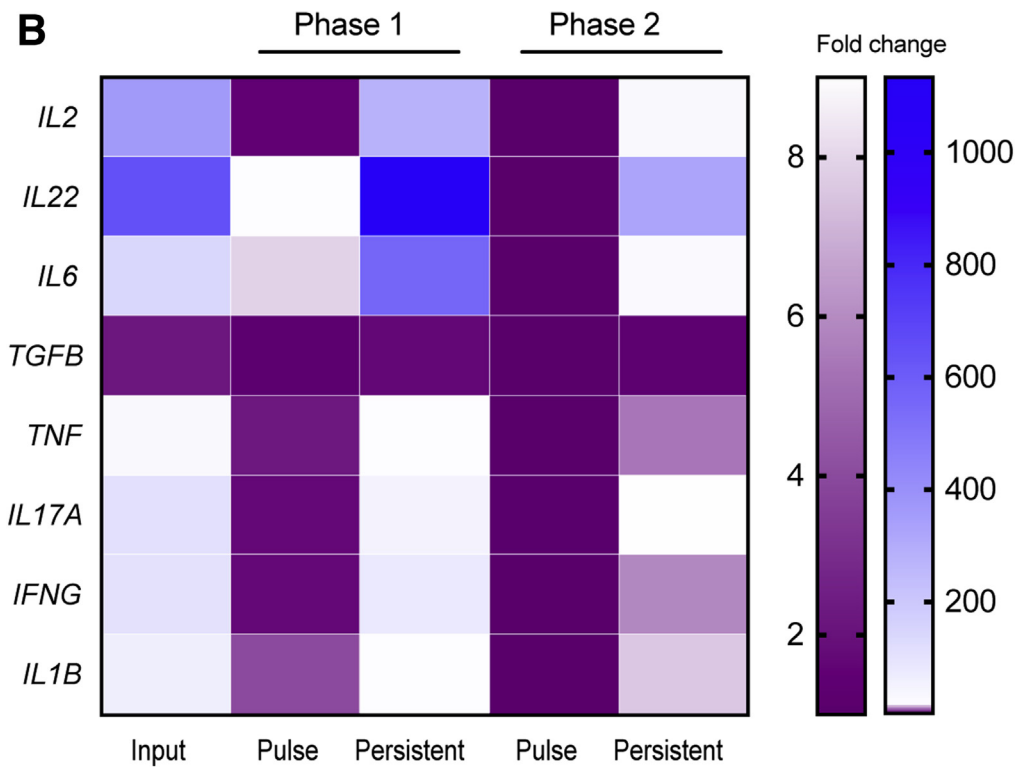


Figure 4. Expression of surface proteins and cytokines by pulse-activated and persistently activated T cells after co-culture with an intestinal epithelial monolayer. (A) Expression of the activation markers CD69 and CD25 and gut-homing receptor integrin β 7 in pulse-activated and persistently activated T cells in phase 1 (P1) and phase 2 (P2) was assessed by flow cytometry. Untreated T cells and T cells after 48 hours of activation with anti-CD3/CD28 Dynabeads (Input) were stained as controls. (B) RNA expression of cytokines from input and pulse-activated T cells harvested 8 hours before the phase 1 peak and persistently activated T cells harvested 24 hours before the end of phase 2 was measured by reverse-transcription quantitative polymerase chain reaction, normalized to unstimulated T cells.



intracellular cytosolic staining pattern (Figures 8 and 9). In phase 2, we also observed an increase in claudin-1 and claudin-4 staining at the apical surface (Figures 7A and 9A). Overall, these findings indicate that not only do activated T cells stimulate the expression of claudin-1 and claudin-4 in an epithelial monolayer, they induce their relocation.

Similar to claudin-1 and claudin-4, claudin-2 contributes to TJ assembly; upon T cell co-culture, claudin-2

preferentially localizes to TJ strands. However, in phase 2, the claudin-2 staining pattern appears to be scattered and disorganized, most notably in the presence of persistently activated T cells (Figure 10). Co-culture with pulse-activated or persistently activated T cells dramatically decreases the occludin mobile fraction and lateral/cellular subpool and favors accumulation into the TJ complex in phase 1 (Figure 7D). In phase 2, the pulse-activated culture showed

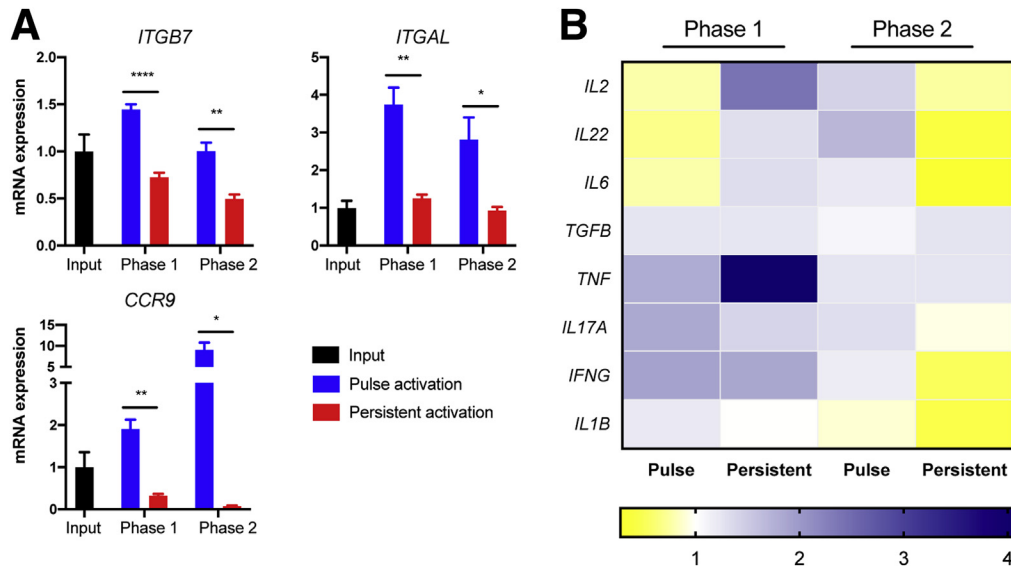


Figure 5. Co-culture of T cells with an epithelial monolayer modulates the expression of gut-homing markers and cytokines differently based on the activation status of the T cells. (A) RNA expression of integrin $\beta 7$, integrin αL , and chemokine receptor C-C Motif Chemokine Receptor 9 measured by reverse-transcription quantitative polymerase chain reaction in activated T cells that had been co-cultured with an epithelial monolayer at the end of phase 1 or phase 2 ($n = 3-4$). The data were normalized to 18S RNA, and T cells immediately after anti-CD3/CD8 activation without co-culture (Input) were used as the baseline to calculate the fold change in expression ($n = 3$). (B) A heatmap showing the ratio of T-cell cytokine mRNA expression between pulse-activated and persistently activated T cells co-cultured with a Caco-2 monolayer and those harvested at the time equivalents of 8 hours before the phase 1 peak and 24 hours before the end of phase 2 without co-culture, where down-regulation is shown in yellow and up-regulation is quantified in blue. * $P \leq .05$; ** $P \leq .01$; **** $P \leq .0001$. ITGB7, integrin beta 7; ITGAL, integrin alpha L.

an increased mobile fraction and lateral/cellular subpool of occludin, whereas with persistent activation occludin levels in the TJ complex were decreased and the subpool depleted (Figures 7D and 11). We detected higher intracellular punctate occludin staining, especially in phase 2 of the pulse-activated culture and both phases of the persistently activated model (Figure 7D), possibly reflecting a mechanism for the relocalization or degradation of the mobile lateral subpool.

There is no difference in ZO-1 staining under any co-culture conditions, reflecting its role as an intracellular protein binding to the C-terminus of transmembrane TJ proteins (Figure 12). There was one additional and intriguing feature shown in this analysis. In the persistently activated co-cultures in phase 2, there was a notable loss of the actin signal (Figure 13A and B). This finding indicates that the interaction of actin with TJ proteins and the apical brush-border microvilli, which are actin-based protrusions, is disrupted or abnormal in the setting of an inflammatory T-cell signal, consistent with reports from IBD intestinal epithelium.¹⁷

Contribution of Epithelial Cell Morphology to Paracellular Permeability

The complexities shown by our analysis of TJ mRNA expression, protein levels, and immunofluorescent patterns in a monolayer exposed to activated T cells suggest that

studying the overall junctional complex in isolation may not provide an exact depiction of the forces that regulate barrier integrity. Classically, an increase in claudin-1 and claudin-4 levels decreases the permeability of the barrier through their sealing function, while excess claudin-2 typically increases permeability through the pore pathway. Thus, the changes in TJ proteins may not explain why there was a reduction in ion flux via the pore pathway (Figure 2B) in phase 1 and a decrease in quality of the leak and unrestricted pathway in phase 2 with persistently activated T-cell exposure (Figure 2D). In addition to the contribution of TJs, permeability of the barrier was affected by cell morphology.⁶ Immunofluorescence staining for claudin-1 showed a noticeable decrease in the height of the epithelial monolayer in phase 1 after co-culture with both pulse-activated and persistently activated T cells (Figure 7A and B). This shortening of the cells was reversed in phase 2. Thus, when considering the mechanisms of barrier function, one also must consider possible changes in cell morphology.

Co-culturing the monolayer with activated T cells decreased the number of cells per microscopic field in both phases (Figure 14A and B), coincident with the down-regulation of Ki67 expression, a marker for cell proliferation (Figure 14C), indicating an inhibition of epithelial cell growth or recovery. Notably, this decrease in cell number and corresponding flattening of the cells (Figure 7A) occur in phase 1, consistent with the observed increase in TER. We conclude that these shortened, fatter cells with decreased

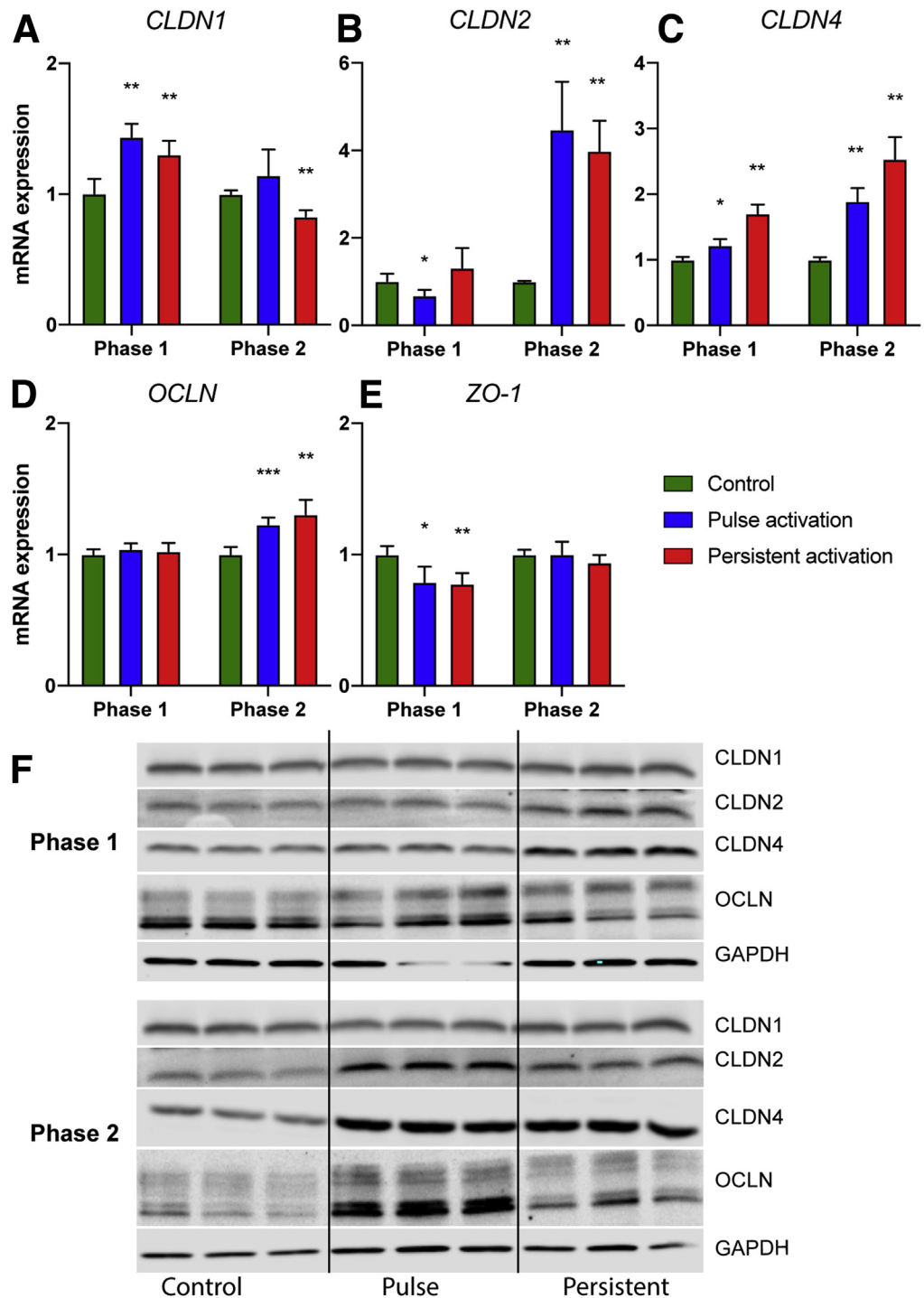
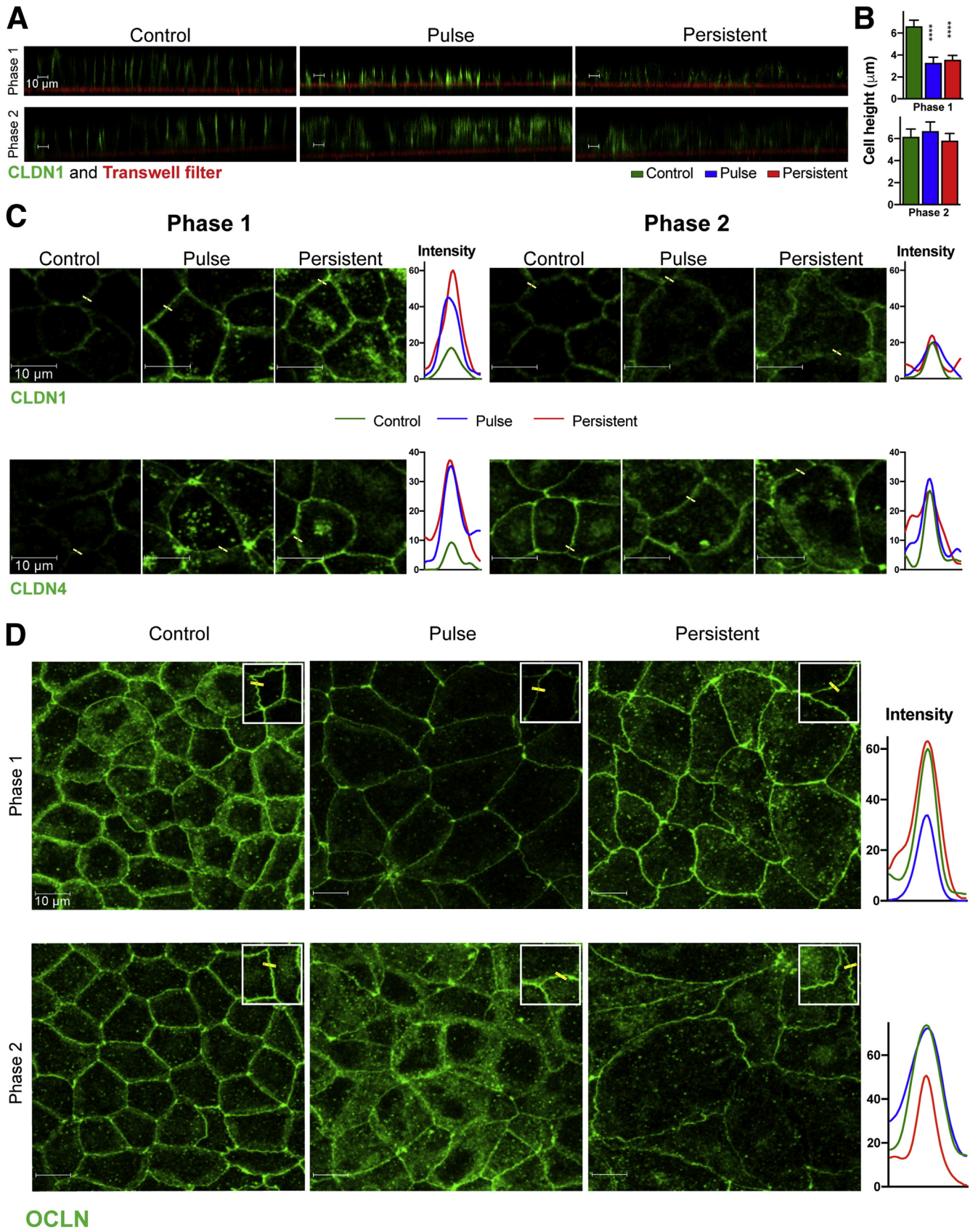


Figure 6. Exposure of an epithelial monolayer to activated T cells modestly regulates the expression of TJ mRNA and proteins. (A–E) RNA expression of claudin-1, -2, -4, occludin (OCLN), and ZO-1 in a monolayer co-cultured with activated T cells at the end of phase 1 or phase 2 ($n = 3-4$). Protein expression by immunoblot of claudin-1, -2, -4, and occludin in a Caco-2 monolayer co-cultured with activated T cells at the end of phase 1 or phase 2. Glyceraldehyde-3-phosphate dehydrogenase (GAPDH) expression was used as an internal standard. (F) Results from different Transwells are shown. $*P \leq .05$; $**P \leq .01$; $***P \leq .001$.

cell membrane-to-cell membrane contact per unit area account in part for the decrease in paracellular permeability in phase 1. In contrast, in phase 2, co-culture with persistently activated T cells induced cell death, as shown by increased DNA staining by the cell-impermeant viability indicator: ethidium homodimer-1 (Figure 14D). In addition, in both phases of co-culture with persistently activated T cells, calcium flux may be disrupted owing to the up-regulation of

Transient Receptor Potential Cation Channel Subfamily V Member 6, a calcium influx protein channel, and down-regulation of the PMCA1b channel, encoded by the *ATP2B1* gene, which extrudes calcium (Figure 14E). These results indicate that in a persistently activated T cell co-culture (ie, an inflammatory setting), prolonged incubation disrupts TJ protein gene expression, alters TJ assembly, induces TJ protein degradation and entry into the cytosol,



distorts cell morphology, and promotes cell death, thus dramatically increasing the unrestricted pathway and leading to high barrier permeability.

Reciprocity in the Mucosa: IECs After Contact With Activated T Cells May Modulate Innate and Adaptive Inflammatory Responses

A key hallmark of the intestinal mucosa is bidirectional host defense regulation between the surface epithelium and the underlying lamina propria immune cells. We investigated if co-culture with either pulse-activated or persistently activated T cells induces a functional immune phenotype within the monolayer. As an example, helper T cell (Th)17 cells play a critical role in the mucosa against extracellular pathogens by regulating the integrity of the epithelial barrier.¹⁸ Because TGF- β , interleukin (IL)6, and IL1 β contribute to the polarization of Th17 cells, we studied their expression in these co-culture models (Figure 15A). Expression of TGF- β and IL1 β mRNA by the monolayer is induced by pulse-activated and persistently activated T cells in both phases, suggesting the presence of an immunologic feedback mechanism, by which activated T cells engage the epithelium to increase its immunoregulatory function.

Because both TGF- β and IL1 β must be processed proteolytically into an active form, we also measured active protein in the conditioned media from these co-culture assays using commercially available paired antibodies. Secretion of active IL1 β was below the limit of detection. TGF- β is a well-known key regulator of epithelial regeneration and a product of both T cells and IECs. The active form of TGF- β accumulated predominantly at the apical surface (Figure 15B). As shown with mRNA measurements, its synthesis is induced by both pulse-activated and persistently activated T cells, apart from persistently activated T cells at the end of phase 2, which may reflect IEC death at this time point (Figure 15B). Activated T cells in isolation secrete minimal amounts of active TGF- β (data not shown).

This proposed reciprocity was confirmed when the expression of molecules related to the capacity for antigen presentation was profiled (Figure 15A). Expression of the inhibitory costimulatory molecule programmed death ligand 1 (PD-L1), the principal ligand of PD-1, is induced in both phases 1 and 2 by persistently activated T cells, while β 2-microglobulin (B2M), a component of the MHC class I system, was up-regulated on the monolayer after co-culture with both types of activated T cells (Figure 15A). Consistent

with the stimulation of B2M in the monolayer, cluster of differentiation 1d and HLA-C also are up-regulated, with slightly different kinetics. Thus, the ability of IECs to present antigen to CD8+ T cells is enhanced in response to T-cell engagement. Ironically, HLA-major histocompatibility complex, class II, DM alpha is down-regulated in the same monolayer, indicating reduced antigen presentation to CD4+ T cells. Although clarification of this dichotomy requires further investigation, overall these results highlight the bidirectional communication between T cells and the epithelium as they work together toward host defense.

Discussion

Chronic inflammation of the gastrointestinal tract often is associated with the loss of epithelial barrier integrity and resultant microbial translocation, as shown in many diseases that include IBD, irritable bowel syndrome, and human immunodeficiency virus infection.^{16,19,20} Events that contribute to the pathology associated with intestinal permeability include the following: (1) direct damage to the epithelium, (2) dysbiosis of the luminal microbiome, and (3) local mucosal inflammation, with an important role for T-cell activation in disease progression and tissue damage.^{21,22} Earlier reports showed that a single cytokine, such as TNF- α or interferon- γ (IFN- γ), can modulate the integrity of the intestinal barrier through alteration of TJ composition, owing to increased expression of incompatible claudin isoforms that exchange with the mobile fraction and lateral/cellular subpool.^{23–25} However, the dynamics of interaction between the epithelium and the underlying immune cells are far more complex than secretion of a single cytokine, and the cooperative, mutually beneficial communication between the 2 compartments must be evaluated. Therefore, we established 2 anatomically correct co-culture models, one in 2 dimensions and another in 3 dimensions, which enable us to characterize the dual effects of distinctly activated T cells on the function of the epithelial barrier as well as the corresponding potential effect of the epithelium on the subjacent immune cells.

Results from our in vitro models show that the capacity of activated T lymphocytes to modulate the integrity of an intestinal barrier is complex and depends on the activation state of the T cell and the kinetics of the cell-cell communication. These perturbations in paracellular permeability induced by activated T cells control both the leak and pore pathways, and may, under specific conditions, also change

Figure 7. (See previous page). Activated T cells reduce the height of an epithelial monolayer in phase 1 and modulate the arrangement of TJ strands and the location of TJ proteins. (A) Both pulse-activated and persistently activated T cells reduce the cell height of a Caco-2 monolayer in phase 1, as shown by claudin-1 (CLDN1) staining (green) (aspect ratio, 5.7:1). The red line is a reflection of phalloidin staining from the Transwell filter. Scale bar: 10 μ m. (B) Cell height was quantified using ImageJ software (National Institutes of Health, Bethesda, MD). (C) Immunofluorescence staining for CLDN1 and CLDN4 in TJ strands in co-culture with activated T cells at the end of phase 1 or phase 2, shown by an image of the top approximately 20% of the x-z slices close to the apical surface. The intensity profile represents a scan of the signal strength shown by the yellow bar. (D) Immunofluorescence staining for occludin (OCLN) in TJ strands and the mobile lateral subpool, in co-culture with activated T cells at the end of phase 1 or phase 2, shown by a total Z stack representation. The sharp, solid green strand is the TJ, the fuzzy, diffuse staining is the mobile lateral subpool. The intensity profile represents a scan of the signal strength shown by the yellow bar in the squares marked in the upper right of each image.

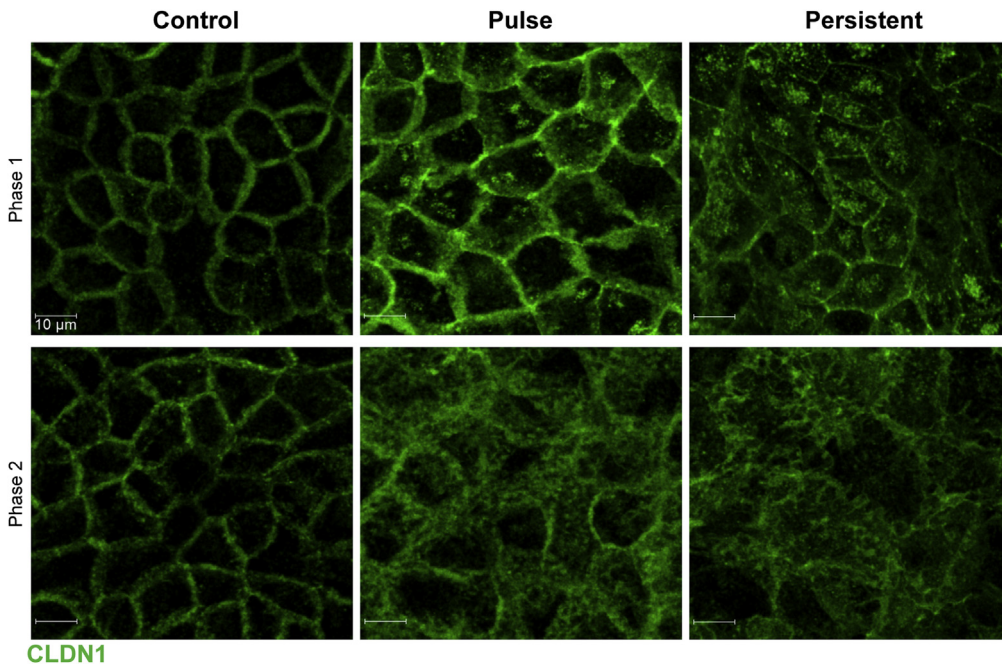


Figure 8. Activated T cells modulate the arrangement of TJ strands and the location CLDN1 Immunofluorescence staining for CLDN1 in TJ strands and the mobile lateral subpool, in co-culture with activated T cells at the end of Phase 1 or Phase 2, shown by a total Z stack representation. The sharp, solid green strand is the TJs; the fuzzy, diffuse staining is the mobile lateral subpool. The scale bar represents 10 μm .

the morphology and health of the monolayer and thereby enhance the unrestricted pathway. One may perceive a drawback of this report is the use of blood-derived T cells, but that choice was intentional because of the proven migration of these cells to the gut during acute and chronic inflammatory disease. When we evaluated the ability of activated blood T cells to express gut chemokine and homing receptors, we found that C-C Motif Chemokine Receptor 9 and the $\beta 7$ chain that associates with integrins $\alpha 4\beta 7$, $\alpha E\beta 7$, and $\alpha L\beta 7$ are induced and differentially regulated in pulse-activated vs persistently activated T cells, possibly explaining their divergent ability to migrate toward colonic spheroids, as shown in [Figure 1](#) and the [Supplementary movies](#). A highly effective treatment for IBD is administration of a blocking antibody to the $\alpha 4\beta 7$ integrin that directs T-cell homing to the gut.²⁶

Initial Contact With Activated T Cells Strengthens Barrier Integrity: Phase 1

Increased TER of the monolayer upon co-culture with either pulse-activated or persistently activated T cells reflects a reduction in ion flux through the pore pathway regulated by the TJ complex. Because conductance through the cell is sufficiently low owing to the high resistance of the plasma membrane, the paracellular pathway normally dictates the overall TER. However, when the cell membrane is perturbed by an external stimulus, cell morphology may cause a consequential contribution to the TER.²⁷ A monolayer with larger cells has a lower percentage of its cell surface shielded by the TJ complex through which ions can pass. Thus, a monolayer with larger cells that has maintained a TJ complex with similar electrical properties will show a higher TER owing to less ion flux. Because the

untreated monolayer established a sturdy leak pathway with limited molecular flux, our model was unable to show if the leak pathway also tightened upon exposure to activated T cells. Thus, we are unable to state unequivocally that TJ structure or composition alone contributed to the increased TER. As seen in phase 1, expression of TJ mRNA, proteins, and their subcellular localization, after either pulse-activated or persistently activated T-cell co-culture, showed no predictable pattern of claudin or occludin use or location to fully explain the increased resistance. Immunofluorescence staining of the TJ proteins, claudin (CLDN)1, CLDN2, CLDN4, occludin, and ZO-1, showed that TJ strand intensity and its ratio to the highly mobile/low-stability protein subpool varied dramatically for each condition and each targeted protein. However, there is a clear accumulation of occludin at the tricellular junction, which may contribute to a strengthened barrier. Furthermore, the slight difference in ZO-1 staining in phase 1 documented in [Figure 12](#) resembles that seen with silencing of Hypoxia Inducible Factor 1B,²⁸ suggesting that one mechanism by which activated T cells may regulate the barrier is by inducing hypoxia or metabolic changes in the IEC. One additional consistent parameter was the decreased number of cells per unit area in the monolayer in phase 1. We propose that lower cell density, in combination with changes in the pore and leak pathway, yielded the higher resistance.

This loss of cells, coupled to their increase in breadth and reduction in height, indicates a major change in cell morphology. The alteration in morphology likely required a rearrangement of new TJs for the expanded cell boundary. It is possible that some of the observed changes in mRNA and protein expression for claudin proteins and occludin may have been in response to these morphologic demands.

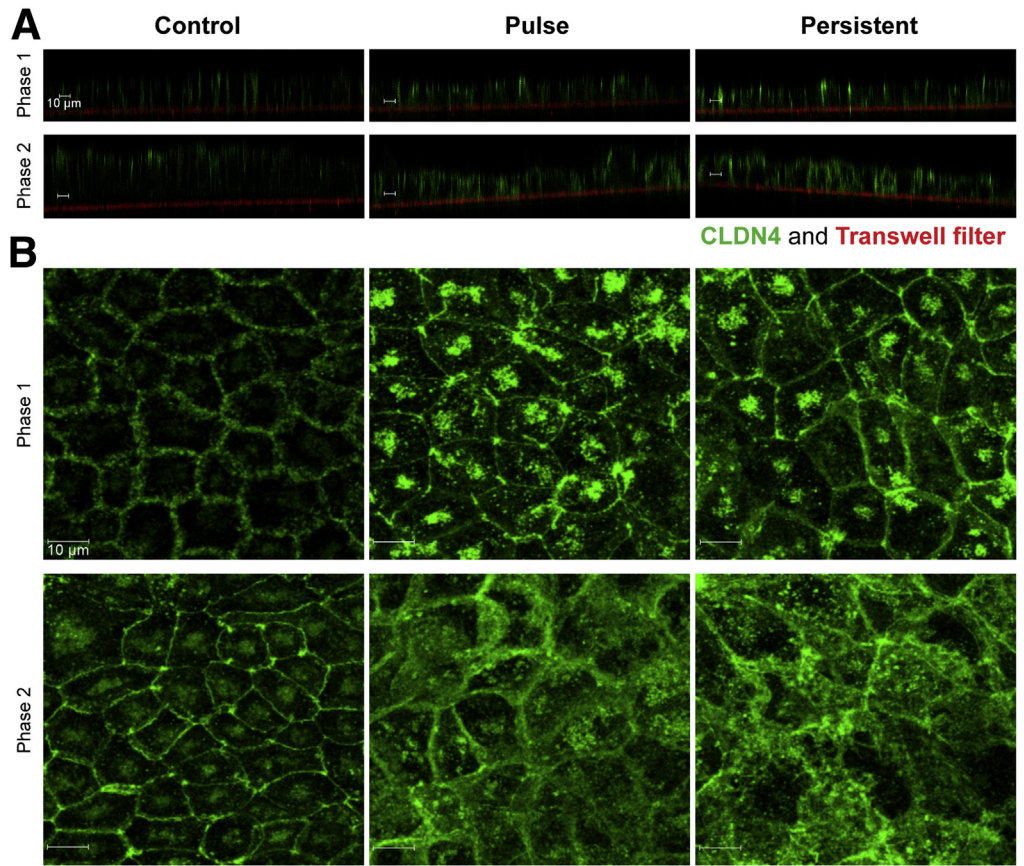


Figure 9. Activated T cells reduce the height of an epithelial monolayer in phase 1 and modulate the arrangement of TJ strands and the location of claudin-4 (CLDN4). (A) Both pulse-activated and persistently activated T cells reduce the cell height of a Caco-2 monolayer in phase 1, as shown by CLDN4 staining (green) (aspect ratio, 5.7:1). The red line is a reflection of phalloidin staining from the Transwell filter. (B) Immunofluorescence staining for CLDN4 in TJ strands and the mobile lateral subpool, as described in the legend for Figure 7.

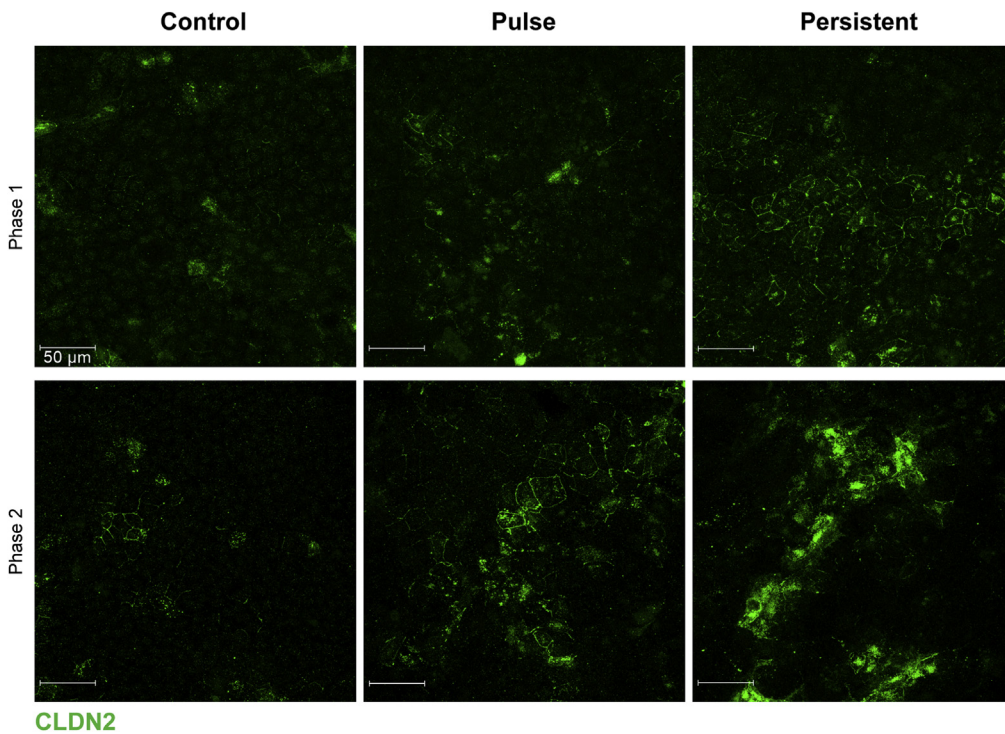


Figure 10. Activated T cells modulate the arrangement of TJ strands and the location of claudin-2 (CLDN2). Immunofluorescence staining for CLDN2 in TJ strands, as described in the legend to Figure 8.

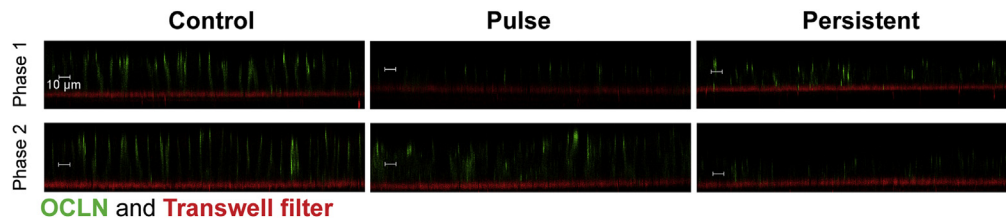


Figure 11. Activated T cells reduce the height of an epithelial monolayer in phase 1, as shown by staining for occludin (OCLN). Both pulse-activated and persistently activated T cells reduce the cell height of a Caco-2 monolayer in phase 1, as shown by OCLN staining (green), as described in the legend for Figure 7.

Combining the changes in morphology with the decreased expression of the proliferation marker Ki67 in phase 1 for both modes of T-cell activation suggests that activated T cells induced the differentiation and morphogenesis of the epithelium and remodeling of the TJ, which stimulated a strengthening of the intestinal barrier function. These results underscore that an acute proinflammatory microenvironment may lead to enhanced host defense and reduced epithelial permeability.

Long-Term Communication With Activated T Cells Yields Dichotomous Changes in Barrier Permeability Depending on the Character of the Immune Stimulation: Phase 2

In the 3-D model and in phase 2 of the 2-D model, barrier permeability evaluated by the leak and unrestricted pathway significantly increased in co-culture with persistently activated T cells. Persistent activation led to a collapse of the 3-D cyst structures and considerable cell death in the 2-D model. The inability of persistently activated T cells to

maintain a strong epithelial barrier is reflected by the observation that pulse-activated T cells rapidly lose their ability for cytokine synthesis in phase 1 and return to a quiescent state, as shown by their decrease in proliferative potential and activation markers. In contrast, persistently activated T cells, upon co-culture maintain, and for some cytokines, increase their rate of synthesis, continue to proliferate, and remain activated. These findings are consistent with the study of cytokines, such as TNF- α or IFN- γ , on 3-D epithelium, which confirms their roles in increasing paracellular permeability via apoptosis or cell shedding.²⁵ In contrast, quiescent, pulse-activated T cells in the 3-D culture modestly affected the leak path, and the increase in the quality of the pore pathway (ie, increased TER) was maintained in phase 2 of the 2-D co-culture. Thus, the pattern of mediators expressed by activated T cells leads to distinct epithelial responses.

A number of factors explain the capacity of persistently activated T cells to increase the flux of ions and molecules through the pore and leak pathways. Immunofluorescence staining highlights a reduction in the

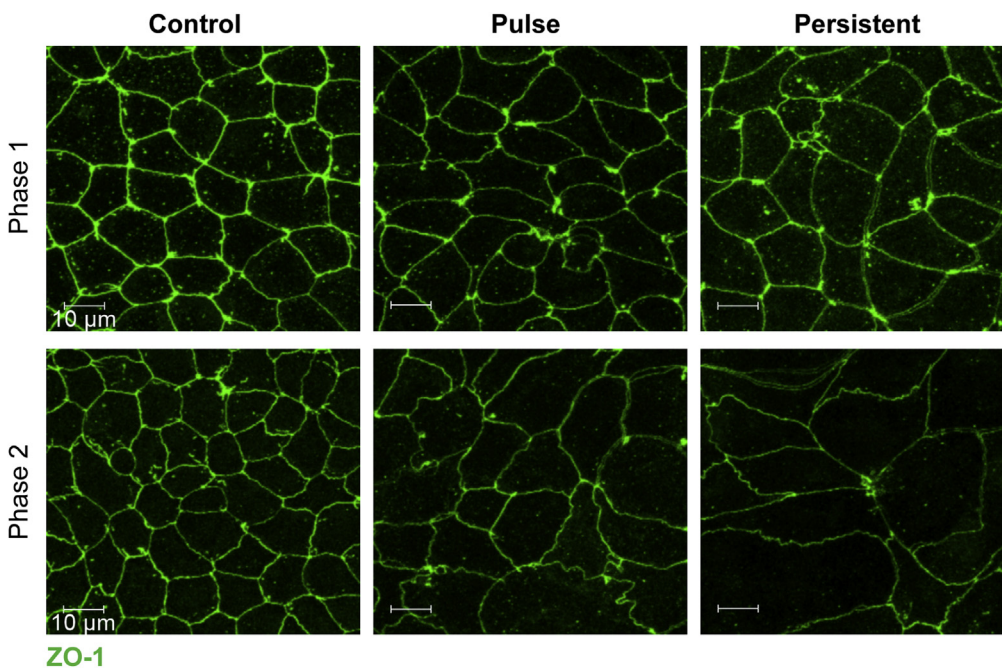


Figure 12. Activated T cells increase the size of the cells within an epithelial monolayer in both phases 1 and 2, as shown by staining for ZO-1. Both pulse-activated and persistently activated T cells increase the cell size in a Caco-2 monolayer at the end of phase 1, and even greater at the end of phase 2, as shown by ZO-1 staining (green), shown by a total Z stack representation.

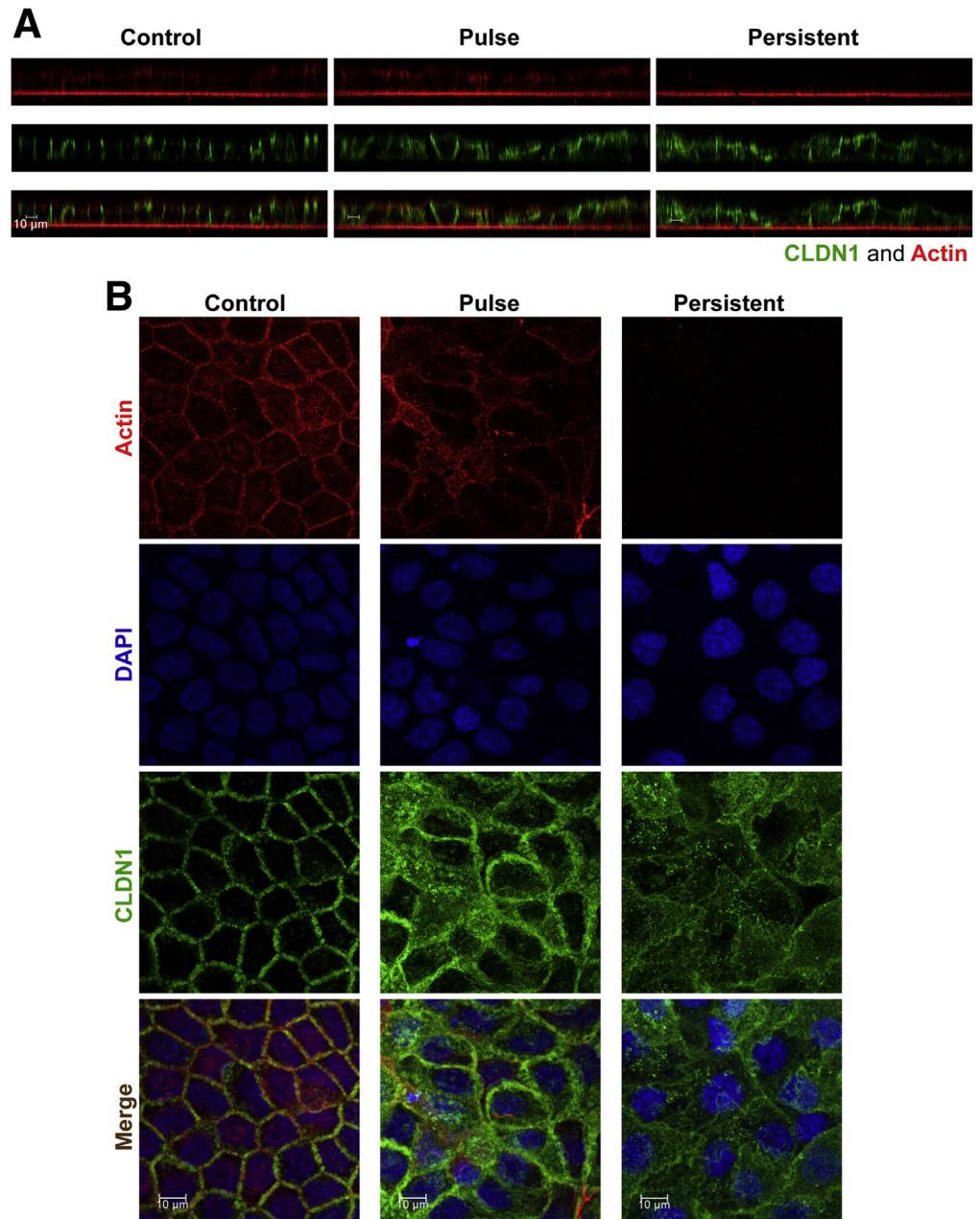


Figure 13. Co-culture of an epithelial monolayer with persistently-activated T cells results in a loss of actin from the microvilli and stimulates a diffuse distribution of CLDN1 from the apical to the basolateral surface in Phase 2. (A) An x-z image of an untreated and treated monolayer (aspect ratio 5.7:1), was stained for actin (phalloidin in red) and CLDN1 (green) in Phase 2. *Top panels* are actin only, *middle panels* are CLDN1, and the *bottom panels* are for co-localization. (B) An image in the x-y plane of a composite Z stack shows colocalization (merged) of actin (red) with CLDN1 (green) in TJ strands in a control monolayer, a slight loss of colocalization in a pulse-activated T cell monolayer co-culture, and a complete loss of the actin signal induced by persistently-activated T cells in Phase 2. DAPI, 4',6-diamidino-2-phenylindole.

intensity of TJ strands after co-culture and higher portion of TJ proteins in the mobile fraction and lateral/cellular subpool, each of which contributes to a leakier epithelium.²³ Our results add a new twist to these findings. The apical brush-border microvilli are an actin-based protrusion, however, the relocation of claudins to the apical surface appears to be accompanied by a dramatic loss in actin staining, indicating that the microvilli structure is disrupted or abnormal in a chronic inflammatory setting. Although it is unclear how the microvilli are altered in patients with IBD, there is clear evidence that the microvilli decrease in length is accompanied by ultrastructural defects.¹⁷ The

inappropriate accumulation of claudin proteins at the apical surface causes us to hypothesize that epithelial polarization is compromised, affecting the architecture of the epithelial barrier.

Persistently activated co-culture conditions also lead to an increase in cell size. Compared with phase 1, the number of cells per unit area reduced from 80% of control to 35%. In addition, persistent activation led to barrier damage owing to cell death and, as a consequence, permeability via the unrestricted pathway allowed free passage of ions, macromolecules, and pathogens. Epithelial cell death and an enhanced unrestricted pathway have been reported previously, induced by cytokines or chronic

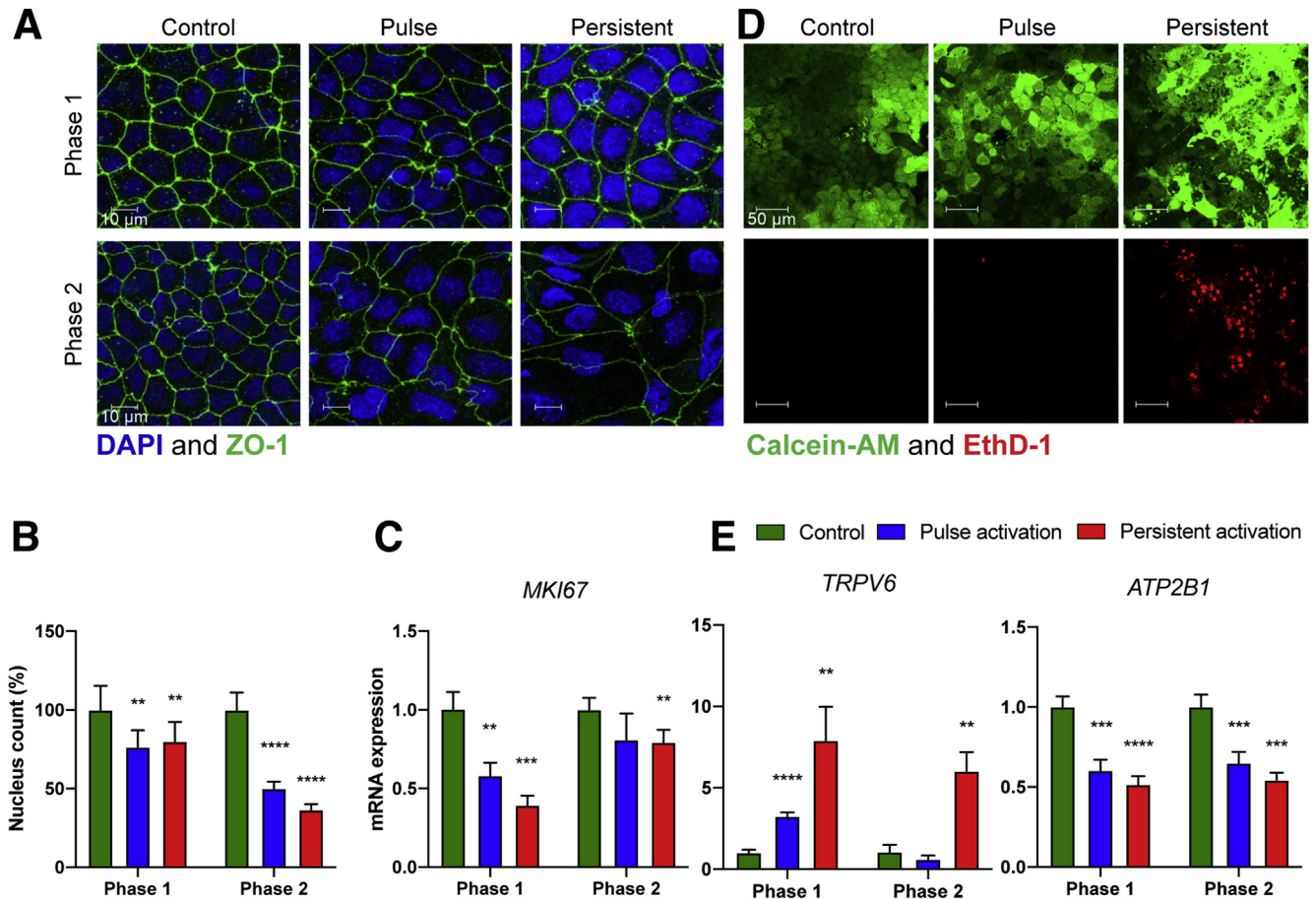


Figure 14. Co-culture with pulse- and persistently-activated T cells increase the size of IECs within a monolayer and persistently-activated T cells induce epithelial cell death. (A) Pulse- and persistently-activated T cells increase the size of Caco-2 cells within a monolayer in Phase 1 and Phase 2, as revealed by ZO-1 staining. (B) Reduced cell number per field ($n = 9-10$ fields), induced by pulse- and persistently-activated T cells, was quantified by counting the number of nuclei detected by DAPI stain. (C) Reduced IEC proliferation, due to pulse- and persistently-activated T cell co-culture, was confirmed by quantifying mRNA expression of the proliferation marker, Ki67 (MKi67). (D) Co-culture with persistently-activated T cells in Phase 2 leads to cell death, as revealed by increased EthD-1 staining. (E) Increased RNA expression of the membrane calcium channel TRPV6, involved in the first step in calcium absorption, and decreased RNA expression of ATP2B1, coding for the PMCA1b channel that functions to remove calcium from the cell, in a Caco-2 monolayer in co-culture with activated T cells at the end of Phase 1 or Phase 2 using TaqMan qPCR, normalized to ribosomal protein, large, P0 as the endogenous control ($n = 3-4$). ** $P \leq .01$, *** $P \leq .001$, **** $P \leq .0001$.

inflammation, as seen in IBD, diverticulitis, and human immunodeficiency virus infection.^{9,29,30} Importantly, microbial translocation, owing to the unrestricted pathway, subsequently initiates chronic systemic immune activation and a sequela of complications in the cardiovascular, liver, coagulation, lipid metabolism, and nervous systems.^{31,32} The mechanism of cell death is unknown, however, it is well established that the accumulation of intracellular calcium is required for the activation of many pathways, including cell death.³³ One possible mechanism, among many others, for cell death in phase 2 might be a result of accumulation of intracellular calcium, owing to the coordinated up-regulation of Transient Receptor Potential Cation Channel Subfamily V Member 6, a calcium influx protein channel, and down-regulation of the PMCA1b channel (*ATP2B1* gene), which extrudes calcium.

Supporting this intriguing possibility, we found that a monolayer in the presence of pulse-activated T cells showed the same potential calcium imbalance in phase 1, but this imbalance was ablated in phase 2, when the monolayer maintained its increased TER and showed no sign of cell death. Although we are unable to propose why a pulse-activated T cell is not lethal, our results do indicate that under an appropriate mode and time of interaction, the barrier may be able to suppress the damage caused by mediators from activated T cells.

Communication With Activated T Cells Modulates the Immune Properties of the Epithelium and Vice Versa

Upon T-cell co-culture, we observed an up-regulation of IL1 β and TGF- β expressed by the epithelial monolayer. TGF-

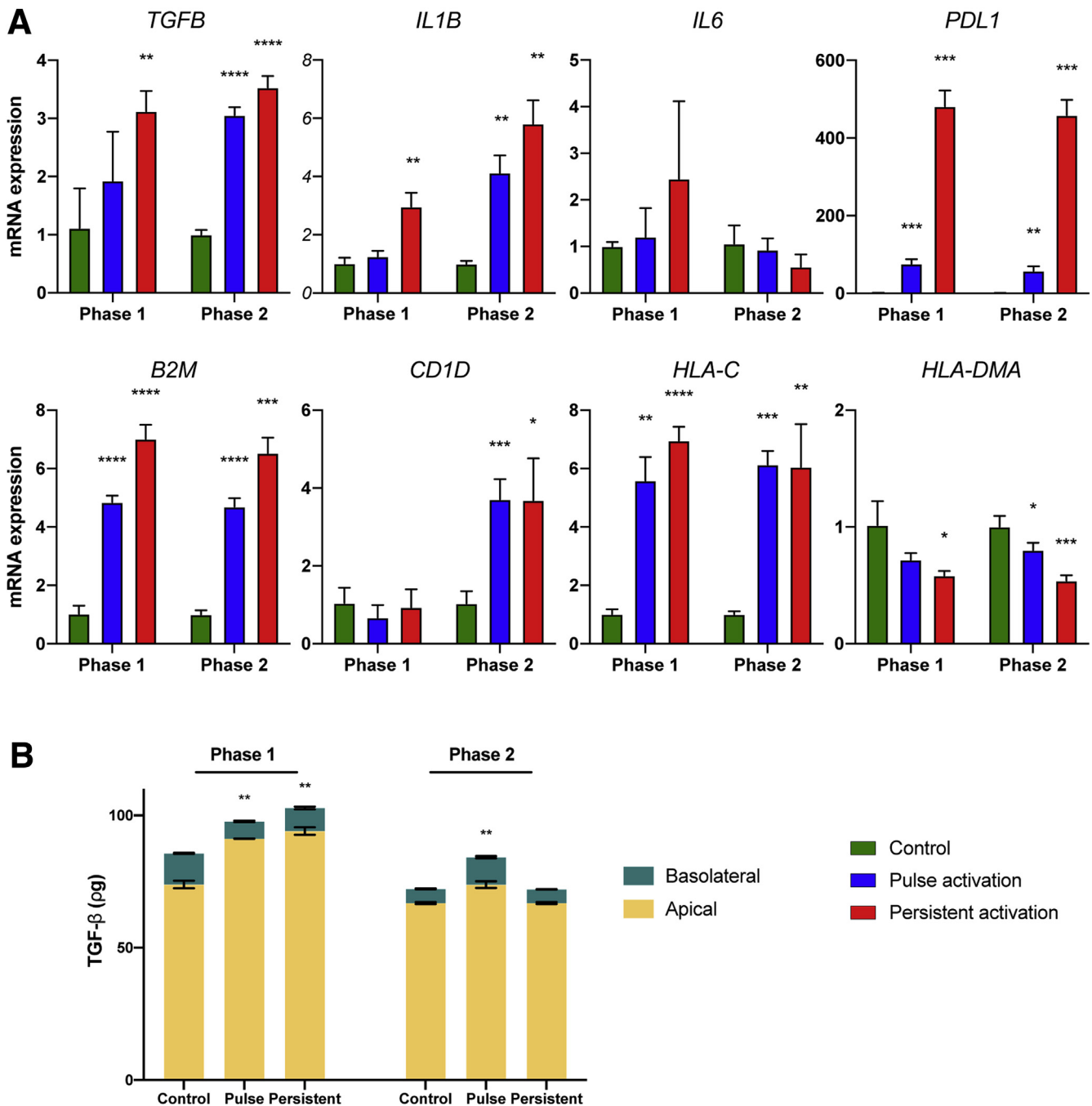


Figure 15. IECs in contact with activated T cells may modulate innate and adaptive inflammatory responses. (A) RNA expression of cytokines, PD-L1, or MHC components in a monolayer co-cultured with activated T cells at the end of phase 1 or phase 2 ($n = 3-4$). (B) Accumulation of active TGF- β in basolateral and apical conditioned media at the end of phase 1 and phase 2 was measured by enzyme-linked immunosorbent assay. * $P \leq .05$, ** $P \leq .01$, *** $P \leq .001$, **** $P \leq .0001$.

β is best known as an immunosuppressive cytokine for its regulatory activity and induction of peripheral tolerance as well as epithelial regeneration, while IL1 β functions as a proinflammatory factor inducing the expansion of differentiated CD4 $^{+}$ T cells and other immune cells. The predominant secretion of TGF- β from the apical surface reflects its critical role in facilitating the recovery of the epithelium

from injury. In a healthy polarized epithelium TGF- β is secreted apically, whereas the type I and type II TGF β receptors are localized specifically at the basolateral surface.³⁴ Disruption of the epithelial barrier by injury enables apically derived TGF- β to activate its receptors via the Smad2-Smad4 complex and initiate the repair process.³⁵ Although there is some evidence that IL1 β and TGF- β are functionally

antagonistic,^{36,37} the production of both cytokines indicates an important, yet unknown, immunoregulatory activity for an activated epithelium.

T-cell cytokine expression was altered in distinct ways when co-cultured with IECs: (1) TGF- β , TNF- α , and IL17A were up-regulated; (2) IL2, IL22, and IL6 were either up-regulated or down-regulated, depending on the activation status and phase; and (3) IFN- γ and IL1 β were down-regulated dramatically in phase 2 during persistent activation, as the monolayer was dying. This complexity of intestinal epithelial-mediated regulation of T-cell cytokine synthesis is consistent with the literature, in which mucosal T cells are distinguished with a unique phenotype that maintains the delicate balance between immune activation and tolerance.³⁸

The expression of PD-L1 increased hundreds-fold with co-culture. PD-L1 was up-regulated in the presence of cytokines such as IFN- γ and TNF- α , during sepsis, and infection. PD-L1 binds to PD-1, which is highly expressed on persistent activated T cells, inhibits T-cell activation, inflammatory cytokine production, and T-cell proliferation and survival, induces the generation of T regulatory cells, and controls inflammation and tolerance in the gastrointestinal tract.³⁹ Recent studies have shown increased PD-L1 expression suppressed Th1 cells in ulcerative colitis, whereas loss of PD-L1 in Crohn's disease contributed to the persistence of Th1 inflammation.⁴⁰ Nevertheless, an increase in PD-L1 in a cytokine-treated Caco-2 monolayer was associated with an increase in epithelial permeability, which can be reversed with a PD-L1 blocking antibody; however, the mechanism still is unclear.

Activated T cells also modulate the expression of MHC-I/II and MHC-I-like molecules on the epithelium. These molecules, when bound to antigen, are important ligands for T-cell survival, development, homeostasis, and activation. In our 2-D model, there was no direct interaction between the epithelium and activated T cells because of the 10- μ m Transwell filter; therefore, modulation of epithelial expression of immune molecules is mediated by soluble factors. Up-regulation of B2M, cluster of differentiation 1d, and HLA-C, and down-regulation of MHC-II, after T-cell co-culture, suggests a role of the activated epithelium in immune tolerance, mediated by the activity of CD8+, CD4+, or natural killer T cells. A recent report showed the expression of MHC-II is higher in Leucine-rich repeat-containing G-protein coupled receptor 5+ epithelial stem cells than in differentiated IECs.⁴¹ Thus, we propose mediators from T cells induce IEC differentiation, accompanied by a reduction in Ki67. Nevertheless, the role for expression of these immunoregulatory proteins to the integrity of the epithelium, host defense, immune tolerance, and homeostasis awaits further study.

Conclusions

We provide mechanistic evidence that IEC T-cell communication modulates epithelial paracellular permeability by regulating TJ assembly and cell morphology and alters the homeostatic immune properties of the epithelium.

These studies will be advanced in the future by evaluating this bidirectional communication using nontransformed epithelial cells as organoid cultures. Overall, our results highlight that in the setting of acute intestinal inflammation the epithelium initially responds by strengthening its barrier function, however, chronic immune exposure disrupts the epithelium, enhancing microbial translocation.

Materials and Methods

Caco-2 Monolayer and TER

Caco-2 BBe cells, a human colorectal adenocarcinoma cell line,⁴² a generous gift from Dr Turner (Harvard Medical School, Boston, MA), were grown in complete medium (RPMI-1640; Corning, Corning, NY), supplemented with 10% fetal bovine serum (Corning), 20-mmol/L HEPES (Genesee, San Diego, CA), at 37°C and 5% humidified CO₂. Cells were seeded at 20,000 cells/Transwell on 0.33-cm² polyester Transwell filters with 0.4- μ m pores (Corning) on the underside of the Transwell filter and allowed to attach for 1 day before the Transwell filter was flipped and cultured in the normal configuration. Permeability was determined measuring TER with a voltohmmeter (World Precision Instruments, Sarasota, FL). TER values were corrected by subtracting a reading obtained from an empty Transwell and multiplied by the area of the filter (Ω cm²). Medium was replenished every 2–3 days for 2 weeks and then daily thereafter. After reaching maturity the TER of the monolayer remained stable for 14 days, during which time the experiment was completed.

Peripheral Blood T-Cell Isolation and Stimulation

Human T cells were isolated from the peripheral blood of healthy donors drawn into heparin-coated tubes using the EasySep Direct Human T Cell Isolation Kit (StemCell, Vancouver, Canada). T cells were rested for 24 hours in complete medium, before activation with anti-CD3/CD28 Dynabeads (ThermoFisher, Waltham, MA) for 2 days. After activation, T cells were washed once. T cells were persistently activated if they were used directly without removing the Dynabeads, or pulse-activated if the Dynabeads were removed using magnetic separation before co-culture.

Caco-2 Cell-T-Cell Co-culture

Activated T cells were suspended in complete medium and added to the upper chamber at 0.5 million/Transwell. The upper and lower chambers were filled with 200 μ L and 1000 μ L media, respectively. TER was measured 3–4 times during the first 24 hours, then once per day. Medium was replenished daily by replacing half of the medium in the upper chamber and all of the medium in the lower chamber.

Flux Through the Monolayer

Monolayers were washed several times with complete media to remove the T cells and incubated with a mixture of 3 dyes in the lower chamber (apical surface): 31.2 μ mol/L fluorescein (Sigma-Aldrich, St. Louis, MO), 78 μ mol/L CF-350-labeled 3.5 kilodaltons dextran (Biotium, Fremont, CA),

and 156 $\mu\text{mol/L}$ TRITC-labeled 70 kilodaltons dextran (ThermoFisher). Every 2 hours, 50 μL from the upper chamber (basolateral surface) was transferred to a black 96-well plate, and the fluorescence intensity was measured using the Victor 3V 1420 fluorescence plate reader (Perkin Elmer, Waltham, MA). The 50 μL of sampled media was returned to the culture plate to maintain equilibrium. Both the ratio of fluorescein or 3.5 kilodaltons dextran flux relative to 70 kilodaltons dextran and the net permeability flux are presented.

Calculation of Apparent Permeability

The apparent permeability (cm/s) of each probe is calculated using the following equation $P_{app} = \frac{dQdt}{C_0A}$, where P_{app} is the apparent permeability, $dQdt$ is the permeability rate (mmol/s), A is the surface area of the filter (cm^2), and C_0 is the initial concentration in the donor chamber (mmol/L).⁴³

Caco-2 Microspheres and Dextran Flux

Fully dispersed 4×10^3 Caco-2 BBe cells were mixed with 100 μL of cold 80% (v/v) Matrigel and grown in a number 1.5 glass-bottom 24-well plate (Mattek Corp, Ashland, MA) for 2–3 weeks to allow microspheres to form. Medium was refreshed every 2 days. The outside of the spheres (the basolateral surface) was exposed to 150 mmol/L FD4 (Sigma-Aldrich) in complete medium. Similarly sized, well-developed cysts were chosen randomly for analysis without bias for their position in the Matrigel layer. Live imaging was performed on a Leica (Wetzlar, Germany) SP8 confocal microscope in a humidified incubator at 37°C. Images were taken every 10 minutes. Fluorescence intensity on the luminal side (interior of the sphere) and basal medium was determined and expressed as a ratio. The change in the fluorescence ratio over time was used to calculate the slope, representing the rate of dextran influx.²⁵

Immunoblotting

Caco-2 monolayers were washed once in situ with Hank's balanced salt solution (HBSS), and the cells were lysed and removed from the Transwell filter with 50 μL RIPA buffer (ThermoFisher), supplemented with Halt Protease and Phosphatase Inhibitor Cocktail, EDTA-free (ThermoFisher). After homogenization by vortexing, the lysates were mixed with reducing sample buffer (ThermoFisher) and boiled for 5 minutes. Proteins were fractionated on a 12% or 14% polyacrylamide gel by electrophoresis and electrotransferred onto a polyvinylidene difluoride membrane (Immobilon-PSQ polyvinylidene difluoride; Millipore Sigma, Burlington, MA). The immunoblot was developed using the same antibodies as immunofluorescence staining and IRDye 800CW donkey anti-rabbit or anti-mouse IgG (H + L) (LI-COR, Lincoln, NE). The membrane was scanned with an Odyssey Imaging system (LI-COR), and the protein concentration in each band was quantified with Image Studio Lite software (LI-COR). The densitometric intensity of each target protein was normalized to the intensity of the glyceraldehyde-3-phosphate dehydrogenase loading control

(mouse anti-human glyceraldehyde-3-phosphate dehydrogenase clone 6C5; Millipore Sigma).

RNA Expression

Caco-2 BBe monolayers were washed in situ with HBSS. Cells attached to the plastic sidewalls of the Transwell were removed before lysis buffer was applied directly to the filter. Resting, pulse-activated, and persistently activated T cells were harvested from the Transwells 8 hours before the phase 1 peak or 24 hours before the end of phase 2 and washed with phosphate-buffered saline (PBS) before RNA isolation. Total RNA was isolated using the Purelink RNA micro scale kit (ThermoFisher) and quantified by Nanodrop (ThermoFisher). A total of 20–40 ng of Caco-2 RNA or 100 ng of T-cell RNA was copied to complementary DNA by reverse transcription using a High-Capacity RNA-to-complementary DNA Kit (ThermoFisher). mRNA levels were quantified using the TaqMan master mix and assays (ThermoFisher) for quantitative polymerase chain reaction. Relative expression was calculated using the $-2^{\Delta\Delta Ct}$ method based on ribosomal protein, large, P0 as the endogenous control for Caco-2 and 18S for T cells.

Immunofluorescence Staining

Caco-2 BBe monolayers were washed twice in situ with HBSS with Ca^{2+} (Lonza, Walkersville, MD) and fixed with paraformaldehyde (0.5% for 30 minutes for TJ proteins or 4% for 20 minutes for actin) at room temperature in 10 mmol/L (2-(N-Morpholino)ethanesulfonic acid, Sigma-Aldrich) pH 6.1, 138 mmol/L KCl, 3 mmol/L MgCl_2 , 2 mmol/L ethylene glycol-bis(β -aminoethyl ether)- N,N,N',N' -tetraacetic acid, and 0.32 mol/L sucrose buffer. The low concentration of paraformaldehyde was used to avoid antigen masking to detect TJ proteins. After washing with HBSS, the Transwell filter was cut from the Transwell insert and placed into a 48-well plate for staining. Monolayers were permeabilized with 0.1% saponin (Sigma-Aldrich) in PHEM buffer (60 mmol/L (1,4-Piperazinediethanesulfonic acid, Sigma-Aldrich), 25 mmol/L HEPES, 10 mmol/L ethylene glycol-bis[β -aminoethyl ether]- N,N,N',N' -tetraacetic acid, and 4 mmol/L MgSO_4 , pH 6.9) for 30 minutes at room temperature, blocked with 10% goat serum (ThermoFisher) for 1 hour at room temperature, then incubated with either rabbit anti-claudin-1 (SAB4200534; Sigma-Aldrich), rabbit anti-claudin-4 (ab53156; Abcam, Cambridge, MA), mouse anti-claudin-2 (32-5600; ThermoFisher), mouse anti-occludin (clone OC-3F10, 33-1500; ThermoFisher), or anti-ZO-1 (33-9100; ThermoFisher) antibody in the presence of 0.05% saponin overnight at 4°C. The signal was shown with either Alexa Fluor 488-conjugated goat anti-rabbit or goat anti-mouse (Jackson ImmunoResearch Laboratories, West Grove, PA) or Alexa Fluor 647-conjugated phalloidin (ThermoFisher) in 0.05% saponin in PHEM buffer for 1 hour at room temperature. The Transwell filter was washed several times with HBSS and mounted in ProLong Diamond Antifade Mountant with 4',6-diamidino-2-phenylindole (ThermoFisher). Imaging was performed with a Leica SP8 confocal microscope, using an oil-immersion 40 \times magnification objective. Z-stack images (0.05- μm thickness)

were analyzed with Leica LAS X software or Fiji.⁴⁴ Aspect ratio for the Z view was 5.7:1, automatically generated by the Leica LAS X software based on the conversion of 1 x-y slice to 1 pixel.

Flow Cytometry

T cells were left untreated, harvested after 48 hours of activation with anti-CD3/CD28 Dynabeads, or collected at the end of phase 1 and phase 2 of co-culture, washed once with PBS, and stained with the Zombie Aqua Fixable Viability Kit (Biolegend), followed by antibody stain: PE/Cy7 anti-human CD69, Brilliant Violet 711 anti-human CD25, fluorescein isothiocyanate anti-human CD4, Alexa Fluor 700 anti-human CD8a, PerCP/cyanine 5.5 anti-human CD3, APC anti-human/mouse integrin $\beta 7$ (all from Biolegend, San Diego, CA). Cells were fixed in 1% paraformaldehyde and analyzed using an LSRFortessa (Becton, Dickinson and Company, Franklin Lakes, NJ) in FACS buffer (0.1% bovine serum albumin, 0.05% sodium azide in PBS). Flow cytometry samples were gated on singlets via standard saline citrate, and then lymphocytes using FSC and standard saline citrate. Gates were drawn to exclude CD14+ CD19+ and dead cells, and expression levels and the percentage of positive cells were quantified using FlowJo v10.4 software (BD).

Expression of Active TGF- β and IL1 β

Media from basolateral and apical chambers were collected at the end of phase 1 and 2 to measure the active forms of TGF- β (Biolegend) and IL1 β (R&D Systems, Minneapolis, MN) by enzyme-linked immunosorbent assay, following the manufacturer's instructions.

Cell Viability

Dead cells were detected by the LIVE/DEAD Viability/Cytotoxicity Kit for mammalian cells after optimization (ThermoFisher).

Statistical Analysis

Statistical analysis was performed using the Brown-Forsythe and Welch analysis of variance for multiple comparisons or the Student *t* test using Prism 8.0 (GraphPad Software, San Diego, CA), as indicated in the Figure legends. All values are provided as means \pm SD. *P* values less than .05 were considered significant.

References

1. Gunzel D, Yu AS. Claudins and the modulation of tight junction permeability. *Physiol Rev* 2013;93:525–569.
2. Shin K, Fogg VC, Margolis B. Tight junctions and cell polarity. *Annu Rev Cell Dev Biol* 2006;22:207–235.
3. Furuse M, Sasaki H, Tsukita S. Manner of interaction of heterogeneous claudin species within and between tight junction strands. *J Cell Biol* 1999;147:891–903.
4. Morita K, Furuse M, Fujimoto K, Tsukita S. Claudin multigene family encoding four-transmembrane domain protein components of tight junction strands. *Proc Natl Acad Sci U S A* 1999;96:511–516.
5. Van Itallie CM, Fanning AS, Bridges A, Anderson JM. ZO-1 stabilizes the tight junction solute barrier through coupling to the perijunctional cytoskeleton. *Mol Biol Cell* 2009;20:3930–3940.
6. Anderson JM, Van Itallie CM. Physiology and function of the tight junction. *Cold Spring Harb Perspect Biol* 2009;1:a002584.
7. Turner JR. Intestinal mucosal barrier function in health and disease. *Nat Rev Immunol* 2009;9:799–809.
8. Van Itallie CM, Holmes J, Bridges A, Gookin JL, Coccaro MR, Proctor W, Colegio OR, Anderson JM. The density of small tight junction pores varies among cell types and is increased by expression of claudin-2. *J Cell Sci* 2008;121:298–305.
9. Tsai PY, Zhang B, He WQ, Zha JM, Odenwald MA, Singh G, Tamura A, Shen L, Sailer A, Yeruva S, Kuo WT, Fu YX, Tsukita S, Turner JR. IL-22 upregulates epithelial claudin-2 to drive diarrhea and enteric pathogen clearance. *Cell Host Microbe* 2017;21:671–681 e4.
10. Yu J, Ordiz MI, Stauber J, Shaikh N, Trehan I, Barnell E, Head RD, Maleta K, Tarr PI, Manary MJ. Environmental enteric dysfunction includes a broad spectrum of inflammatory responses and epithelial repair processes. *Cell Mol Gastroenterol Hepatol* 2016;2:158–174 e1.
11. Okumura R, Takeda K. Roles of intestinal epithelial cells in the maintenance of gut homeostasis. *Exp Mol Med* 2017;49:e338.
12. Kulkarni N, Pathak M, Lal G. Role of chemokine receptors and intestinal epithelial cells in the mucosal inflammation and tolerance. *J Leukoc Biol* 2017;101:377–394.
13. Allaire JM, Crowley SM, Law HT, Chang SY, Ko HJ, Vallance BA. The intestinal epithelium: central coordinator of mucosal immunity. *Trends Immunol* 2018;39:677–696.
14. Reyes BM, Danese S, Sans M, Fiocchi C, Levine AD. Redox equilibrium in mucosal T cells tunes the intestinal TCR signaling threshold. *J Immunol* 2005;175:2158–2166.
15. Hoytema van Konijnenburg DP, Reis BS, Pedicord VA, Farache J, Victora GD, Mucida D. Intestinal epithelial and intraepithelial T cell crosstalk mediates a dynamic response to infection. *Cell* 2017;171:783–794 e13.
16. Funderburg NT, Stubblefield Park SR, Sung HC, Hardy G, Clagett B, Ignatz-Hoover J, Harding CV, Fu P, Katz JA, Lederman MM, Levine AD. Circulating CD4(+) and CD8(+) T cells are activated in inflammatory bowel disease and are associated with plasma markers of inflammation. *Immunology* 2013;140:87–97.
17. VanDussen KL, Stojmirovic A, Li K, Liu TC, Kimes PK, Muegge BD, Simpson KF, Ciorba MA, Perrigoue JG, Friedman JR, Towne JE, Head RD, Stappenbeck TS. Abnormal small intestinal epithelial microvilli in patients with Crohn's disease. *Gastroenterology* 2018;155:815–828.
18. Kempski J, Brockmann L, Gagliani N, Huber S. TH17 cell and epithelial cell crosstalk during inflammatory bowel

- disease and carcinogenesis. *Front Immunol* 2017; 8:1373.
19. Alzahrani J, Hussain T, Simar D, Palchadhuri R, Abdel-Mohsen M, Crowe SM, Mbogo GW, Palmer CS. Inflammatory and immunometabolic consequences of gut dysfunction in HIV: parallels with IBD and implications for reservoir persistence and non-AIDS comorbidities. *EBioMedicine* 2019;46:522–531.
 20. Liebrechts T, Adam B, Bredack C, Roth A, Heinzel S, Lester S, Downie-Doyle S, Smith E, Drew P, Talley NJ, Holtmann G. Immune activation in patients with irritable bowel syndrome. *Gastroenterology* 2007; 132:913–920.
 21. Stewart AS, Pratt-Phillips S, Gonzalez LM. Alterations in intestinal permeability: the role of the "leaky gut" in health and disease. *J Equine Vet Sci* 2017;52:10–22.
 22. Mu Q, Kirby J, Reilly CM, Luo XM. Leaky gut as a danger signal for autoimmune diseases. *Front Immunol* 2017; 8:598.
 23. Capaldo CT, Farkas AE, Hilgarth RS, Krug SM, Wolf MF, Benedik JK, Fromm M, Koval M, Parkos C, Nusrat A. Proinflammatory cytokine-induced tight junction remodeling through dynamic self-assembly of claudins. *Mol Biol Cell* 2014;25:2710–2719.
 24. Wang F, Schwarz BT, Graham WV, Wang Y, Su L, Clayburgh DR, Abraham C, Turner JR. IFN- γ -induced TNFR2 expression is required for TNF-dependent intestinal epithelial barrier dysfunction. *Gastroenterology* 2006;131:1153–1163.
 25. Juuti-Uusitalo K, Klunder LJ, Sjollem KA, Mackovicova K, Ohgaki R, Hoekstra D, Dekker J, van Ijzendoorn SC. Differential effects of TNF (TNFSF2) and IFN- γ on intestinal epithelial cell morphogenesis and barrier function in three-dimensional culture. *PLoS One* 2011;6:e22967.
 26. Feagan BG, Rutgeerts P, Sands BE, Hanauer S, Colombel JF, Sandborn WJ, Van Assche G, Axler J, Kim HJ, Danese S, Fox I, Milch C, Sankoh S, Wyant T, Xu J, Parikh A, Group GS. Vedolizumab as induction and maintenance therapy for ulcerative colitis. *N Engl J Med* 2013;369:699–710.
 27. Odijk M, van der Meer AD, Levner D, Kim HJ, van der Helm MW, Segerink LI, Frimat JP, Hamilton GA, Ingber DE, van den Berg A. Measuring direct current trans-epithelial electrical resistance in organ-on-a-chip microsystems. *Lab Chip* 2015;15:745–752.
 28. Saeedi BJ, Kao DJ, Kitzenberg DA, Dobrinskikh E, Schwisow KD, Masterson JC, Kendrick AA, Kelly CJ, Bayless AJ, Kominsky DJ, Campbell EL, Kuhn KA, Furuta GT, Colgan SP, Glover LE. HIF-dependent regulation of claudin-1 is central to intestinal epithelial tight junction integrity. *Mol Biol Cell* 2015;26:2252–2262.
 29. Nalle SC, Turner JR. Intestinal barrier loss as a critical pathogenic link between inflammatory bowel disease and graft-versus-host disease. *Mucosal Immunol* 2015;8:720–730.
 30. Allam O, Samarani S, Mehraj V, Jenabian MA, Tremblay C, Routy JP, Amre D, Ahmad A. HIV induces production of IL-18 from intestinal epithelial cells that increases intestinal permeability and microbial translocation. *PLoS One* 2018;13:e0194185.
 31. Troseid M, Manner IW, Pedersen KK, Haissman JM, Kvale D, Nielsen SD. Microbial translocation and cardiometabolic risk factors in HIV infection. *AIDS Res Hum Retroviruses* 2014;30:514–522.
 32. Wiest R, Albillos A, Trauner M, Bajaj JS, Jalan R. Targeting the gut-liver axis in liver disease. *J Hepatol* 2017; 67:1084–1103.
 33. Bagur R, Hajnoczky G. Intracellular Ca²⁺ Sensing: its role in calcium homeostasis and signaling. *Mol Cell* 2017;66:780–788.
 34. Murphy SJ, Dore JJ, Edens M, Coffey RJ, Barnard JA, Mitchell H, Wilkes M, Leof EB. Differential trafficking of transforming growth factor- β receptors and ligand in polarized epithelial cells. *Mol Biol Cell* 2004; 15:2853–2862.
 35. Moyano JV, Greciano PG, Buschmann MM, Koch M, Matlin KS. Autocrine transforming growth factor- β 1 activation mediated by integrin α _v β ₃ regulates transcriptional expression of laminin-332 in Madin-Darby canine kidney epithelial cells. *Mol Biol Cell* 2010; 21:3654–3668.
 36. Hebel K, Rudolph M, Kosak B, Chang HD, Butzmann J, Brunner-Weinzierl MC. IL-1 β and TGF- β act antagonistically in induction and differentially in propagation of human proinflammatory precursor CD4⁺ T cells. *J Immunol* 2011;187:5627–5635.
 37. Benus GF, Wierenga AT, de Gorter DJ, Schuringa JJ, van Bennekum AM, Drenth-Diephuis L, Vellenga E, Eggen BJ. Inhibition of the transforming growth factor β (TGF β) pathway by interleukin-1 β is mediated through TGF β -activated kinase 1 phosphorylation of SMAD3. *Mol Biol Cell* 2005;16:3501–3510.
 38. van Wijk F, Cheroutre H. Mucosal T cells in gut homeostasis and inflammation. *Expert Rev Clin Immunol* 2010;6:559–566.
 39. Francisco LM, Sage PT, Sharpe AH. The PD-1 pathway in tolerance and autoimmunity. *Immunol Rev* 2010; 236:219–242.
 40. Beswick EJ, Grim C, Singh A, Aguirre JE, Tafoya M, Qiu S, Rogler G, McKee R, Samedi V, Ma TY, Reyes VE, Powell DW, Pinchuk IV. Expression of programmed death-ligand 1 by human colonic CD90(+) stromal cells differs between ulcerative colitis and Crohn's disease and determines their capacity to suppress Th1 cells. *Front Immunol* 2018;9:1125.
 41. Biton M, Haber AL, Rogel N, Burgin G, Beyaz S, Schnell A, Ashenberg O, Su CW, Smillie C, Shekhar K, Chen Z, Wu C, Ordovas-Montanes J, Alvarez D, Herbst RH, Zhang M, Tirosh I, Dionne D, Nguyen LT, Xifaras ME, Shalek AK, von Andrian UH, Graham DB, Rozenblatt-Rosen O, Shi HN, Kuchroo V, Yilmaz OH, Regev A, Xavier RJ. T helper cell cytokines modulate intestinal stem cell renewal and differentiation. *Cell* 2018; 175:1307–1320 e22.
 42. Peterson MD, Mooseker MS. Characterization of the enterocyte-like brush border cytoskeleton of the C2BBE clones of the human intestinal cell line, Caco-2. *J Cell Sci* 1992;102:581–600.
 43. Artursson P, Karlsson J. Correlation between oral drug absorption in humans and apparent drug

permeability coefficients in human intestinal epithelial (Caco-2) cells. *Biochem Biophys Res Commun* 1991; 175:880–885.

44. Schindelin J, Arganda-Carreras I, Frise E, et al. Fiji: an open-source platform for biological-image analysis. *Nature Methods* 2012;9:676–682.

Received October 23, 2019. Accepted July 7, 2020.

Correspondence

Address correspondence to: Alan D. Levine, PhD, Case Western Reserve University School of Medicine, Wood W217C, 10900 Euclid Avenue, Cleveland, Ohio 44106-4960. e-mail: alan.levine@case.edu; fax: (216) 368-3055.

Acknowledgments

The authors thank members of Dr Turner's laboratory at Harvard Medical School (Jerrod Turner, Wangsun Choi), Richard Lee of the Case Western Reserve University Neurosciences Confocal Imaging Core, and Dr Charlotte Chung, formerly at Case Western now at Emory University, for their help in data interpretation, assistance with accessing equipment, and for their advice in experimental design and data analysis. All authors provided final approval of the version of the manuscript submitted.

CRedit Authorship Contributions

Nga Le (Conceptualization: Equal; Data curation: Lead; Formal analysis: Equal; Methodology: Supporting; Writing – original draft: Lead; Writing – review & editing: Supporting);

Claire Mazahery (Methodology: Supporting; Writing – review & editing: Supporting; recruiting of participants: Lead);

Kien Nguyen (Data curation: Supporting);

Alan D. Levine (Conceptualization: Equal; Formal analysis: Equal; Funding acquisition: Lead; Methodology: Supporting; Project administration: Lead; Resources: Lead; Supervision: Lead; Writing – original draft: Supporting; Writing – review & editing: Lead).

Conflicts of interest

The authors disclose no conflicts.

Funding

Research was supported by the National Institute of Allergy and Infectious Diseases, National Institute of Mental Health, and National Institute on Drug Abuse of the National Institutes of Health under grants DP1 DA037997, R01AI148083, R01DA043159, R01MH110360, R01DA036171, P30AI036219, and S10-OD016164 (Case Western Reserve University School of Medicine Light Microscopy Core Facility). Also supported by the National Institute of Allergy and Infectious Diseases and National Institute of General Medical Sciences of the National Institutes of Health under grants T32AI089474 and T32GM007250 (C.M.).